



Agenzia nazionale per le nuove tecnologie, l'energia
e lo sviluppo economico sostenibile



Ministero dello Sviluppo Economico

RICERCA DI SISTEMA ELETTRICO

Minimizing temperature difference in HVAC systems for high
energy efficiency in buildings
(IEA – ECBCS Annex 59)

M. Perino, V. Serra, S. P. Corgnati, E. Fabrizio, F. Favoino, S. Fantucci



DIPARTIMENTO ENERGIA

Report RdS/2012/ 117

MINIMIZING TEMPERATURE DIFFERENCE IN HVAC SYSTEMS FOR HIGH ENERGY EFFICIENCY IN BUILDINGS (IEA – ECBCS ANNEX 59)

M. Perino, V.Serra, S. P. Corgnati, E.Fabrizio, F. Favoino, S.Fantucci (Politecnico di Torino Dipartimento Energia)

Settembre 2012

Report Ricerca di Sistema Elettrico

Accordo di Programma Ministero dello Sviluppo Economico – ENEA

Area: Razionalizzazione e risparmio nell'uso dell'energia

Progetto: Studi e valutazioni sull'uso razionale dell'energia: Tecnologie per il risparmio elettrico nel settore civile

Responsabile del Progetto: Gaetano Fasano, ENEA

Indice

Sommario	4
Introduzione.....	4
Descrizione delle attività svolte, risultati, discussione e pubblicazioni.....	7
<i>Approfondimento 1</i>	10
<i>Approfondimento 2</i>	30
<i>Approfondimento 3</i>	44
Conclusioni.....	46
Appendice.....	47

Sommario

I temi sviluppati nell'ambito del presente progetto sono parte del più ampio progetto della International Energy Agency -ECBCS Annex 59 "Minimizing Temperature Difference in HVAC Systems for High Energy Efficiency in Buildings", approvato dall'Executive Committee nel mese di Ottobre 2011. Il gruppo di ricerca TEBE (www.polito.it/tebe) del Dipartimento di ENERGIA del Politecnico di Torino ha avuto un ruolo propositivo e attivo nella definizione dei contenuti del progetto, fin dalla sua fase di concezione, partecipando agli incontri preliminari tra il nucleo dei proponenti e contribuendo alla scrittura del progetto stesso.

In questa fase di start-up del progetto, l'attività dell'unità di ricerca del Politecnico di Torino ha focalizzato il proprio specifico approfondimento sui sistemi per il riscaldamento ambientale basati su impianti solari termici che utilizzano fluidi e sistemi innovativi (con particolare riferimento a materiali a cambiamento di fase fluidizzati, "Slurry PCM"). Questa fase della ricerca è risultata essenziale per cominciare a individuare le effettive possibilità applicative, nonché i limiti, di queste soluzioni tecnologiche integrate. Parallelamente, è stato condotto un approfondimento sulle potenzialità applicative dei pannelli radianti per la climatizzazione accoppiati a sistemi impiantistici operanti a temperatura moderata. Il tema guida della ricerca può essere sintetizzato nell'analisi delle potenzialità applicative di nuovi sistemi integrati del sistema edificio-impianto che interagiscono con la fonte energetica solare.

Gli studi condotti sono propedeutici allo sviluppo di uno specifico modello di calcolo per il progetto di sistemi impiantistici per la climatizzazione, in particolare utilizzando la tecnologia radiante, in presenza di elevati carichi solari.

Introduzione

L'attività di ricerca condotta è strettamente correlata al programma dell'Annex 59 dell'IEA (International Energy Agency) "High Temperature Cooling & Low Temperature Heating in Buildings".

Al fine di inquadrare al meglio le linee di approfondimento del progetto, si riportano di seguito alcuni estratti del documento che illustra il progetto stesso.

"The purpose of buildings and HVAC systems is to maintain suitable indoor climate quality, including required levels of temperature, humidity and indoor air quality. Theoretically, any heating source with a higher temperature than the indoor environment can supply heat in winter and vice versa for cooling sources in summer. Since the temperature of heating sources and cooling sources influences HVAC energy consumption directly, high temperature cooling and low temperature heating has the potential to increase energy efficiency. The concept of reducing the temperature difference between heating sources/cooling sources and the indoor environment typically involves increasing the dimensions of heat exchange surfaces. Independent control of temperature and humidity is another important aspect of high temperature cooling and low temperature heating.

[...] the proposed project is organized following the idea of reducing mixture loss and transfer loss, and the work subtasks are arranged in response to the current insufficiency or inadequateness of HVAC system.

The main objectives of the research proposal can be summarized as three aspects:

- Establish a methodology for analysis of the thermal environment system from the perspective of reducing mixture loss and transfer loss.*
- Develop a new concept for temperature and humidity independent control system*
- Research on radiant terminals and the direction of efficient HVAC system for large space buildings.*

The ultimate goal of the Annex is hence to:

Build up the concept of surveying HVAC system from the perspective of reducing mixture loss and transfer loss then apply it in analysis of actual energy saving technologies

To reach this goal, an international collaboration is needed on different issues: a deep and comprehensive investigation to evaluate current situation, summarize the appropriate and inappropriate design of HVAC systems, unify and clarify the research methodology, discuss on basic settings and methodology of simulation and testing, research on key parameters of radiant terminals, study energy saving potential and limitation of radiant terminals combined with fresh air system, research on HVAC indoor terminals for large space building, including radiant floor and supply air terminals.

La struttura dell'Annex 59 è riportata nella figura 1 allegata.

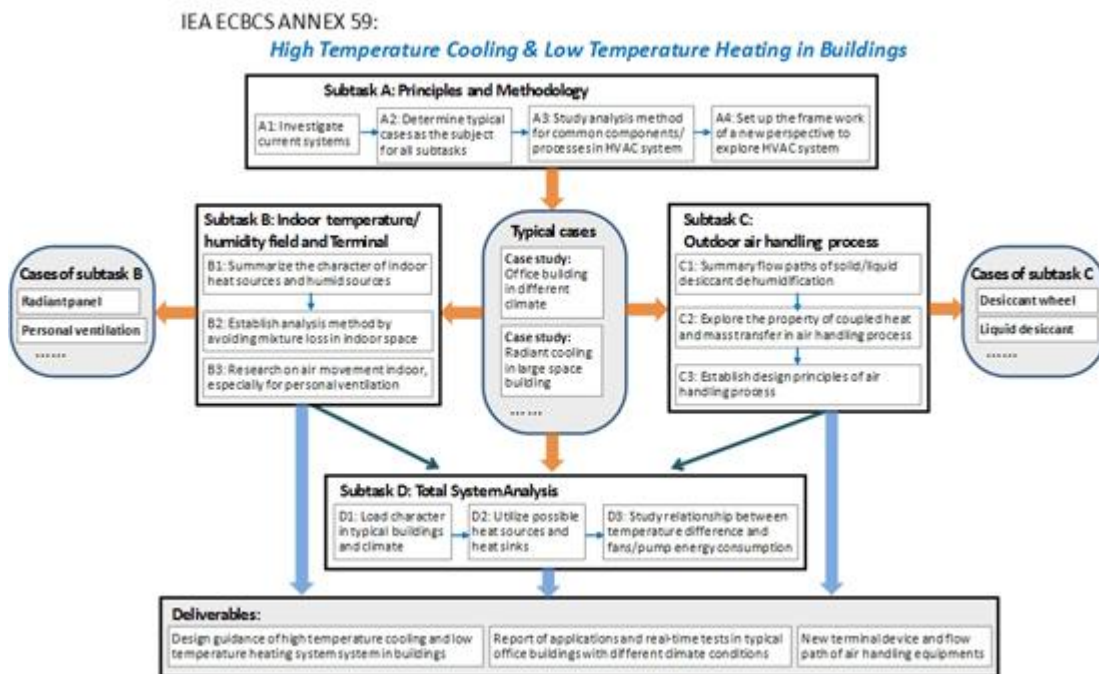


Figura 1 – Struttura dell'Annex 59.

Descrizione delle attività svolte, risultati, discussione e pubblicazioni

Relativamente ai sistemi per il riscaldamento ambientale basati su impianti solari termici che utilizzano fluidi e sistemi innovativi, in questa prima fase delle attività, il lavoro del gruppo di lavoro del Politecnico di Torino si è organizzato su tre fronti distinti:

- analisi della configurazione impiantistica di base,
- analisi e selezione dei fluidi di processo,
- creazione di un profilo temporale “tipo” di carico termico e sviluppo di un modello numerico semplificato per il pre-dimensionamento della superficie captante e dell’accumulo termico.

Il primo fronte ha riguardato la concezione degli schemi di impianto (collettore-circuito primario-accumulo-circuito secondario) da associare al collettore solare a materiale a cambiamento di fase fluidizzato in progetto. In particolare si è svolto uno studio specifico in relazione ai fluidi da adottare per i vari circuiti (slurry-PCM sul primario, slurry-PCM sul primario e secondario con scambiatore intermedio, slurry-PCM sul primario e secondario senza scambiatore intermedio), pervenendo a due schemi tipo riassunti nei disegni seguenti (figure 2 e 3).

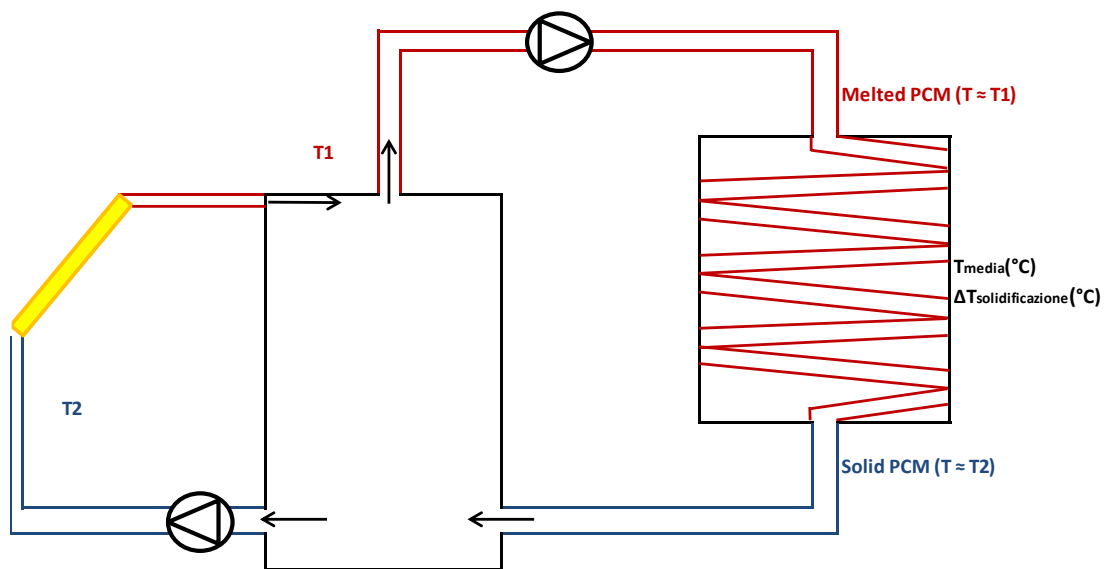


Figura 2 - Schema di impianto solare termico con due circuiti a slurry-PCM aperti.

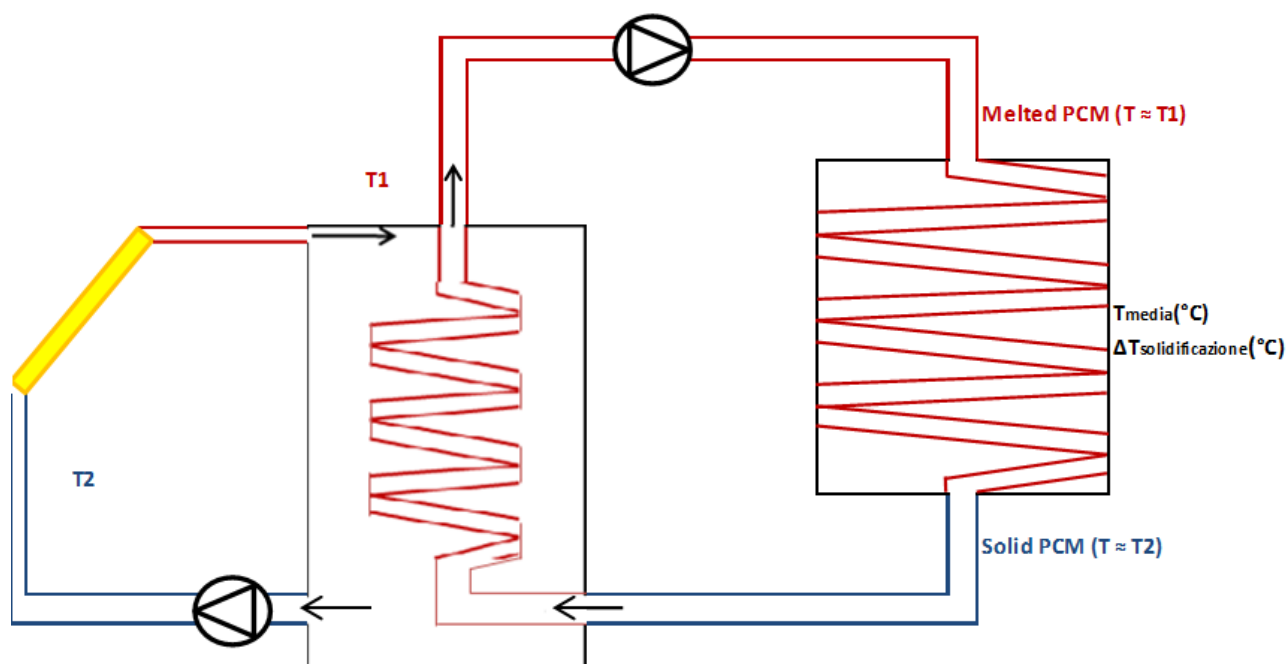


Figura 3 - Schema di impianto solare termico con due circuiti a slurry-PCM chiusi e scambiatore intermedio

Nel primo schema di impianto i due circuiti (primario e secondario dell'utenza) sono collegati idraulicamente all'accumulo sotto forma di slurry-PCM. Il materiale viene fuso nel passaggio nel collettore e, successivamente (se la radiazione solare è sufficientemente alta), passa dalla temperatura T_2 alla temperatura T_1 . Sull'utenza il materiale subisce la solidificazione e ritorna all'accumulo sotto forma di solido (sospeso in fase liquida).

Nel secondo schema, invece, il circuito primario è collegato idraulicamente all'accumulo mentre il circuito secondario dell'utenza è dotato di uno scambiatore intermedio annegato nell'accumulo. Il funzionamento è analogo a quello dello schema precedente con la differenza che in questo caso può essere adottato un fluido diverso per il circuito secondario (ad esempio acqua o uno slurry PCM con caratteristiche termo fisiche diverse da quello del primario).

Da un punto di vista puramente termotecnico il caso migliore e più efficiente è rappresentato dal primo schema poichè utilizza un circuito aperto per la carica e lo scarico dell'accumulo. Senza l'utilizzo di uno scambiatore, la quantità di energia termica che può essere trasferita all'utenza è maggiore.

Tuttavia, è raro che si possa utilizzare in utenze domestiche, ad esempio pannelli radianti a pavimento, la miscela acqua-slurry-PCM che presenta una densità maggiore dell'acqua, anche perché i PCM microincapsulati potrebbero in qualche punto dell'impianto danneggiare o ostruire le tubazioni. L'opportunità di utilizzare il PCM fluidizzato anche sull'utenza dovrà essere oggetto di ulteriori studi, pertanto si è deciso di adottare il secondo schema di impianto con scambiatore intermedio sull'accumulo. Certamente questo secondo schema di impianto risulta essere meno efficiente del primo in quanto nello scambio di energia termica viene "perso" un salto di temperatura di circa 2-3 °C.

Il secondo fronte di attività ha riguardato la selezione del materiale a cambiamento di fase (PCM) fluidizzato più adatto per l'impiego all'interno del collettore solare. Questo studio, riportato nel dettaglio nell'approfondimento 1, ha preso in esame come primo elemento la temperatura di fusione/solidificazione, andando a stimare la quantità di calore

immagazzinabile nella miscela acqua + PCM micro incapsulato da utilizzarsi in progetto in funzione sia del calore specifico del materiale in esame, sia della temperatura media di lavoro rispetto alla temperatura dell'utenza.

Il terzo fronte ha consentito di ottenere un profilo di richiesta termica (ottenuto mediante simulazione numerica con il software Energy Plus). Sulla base di questa informazione è quindi stato possibile andare a simulare il comportamento di massima del sistema captatore accumulo termico e andare ad indagare l'effetto della variazione della temperatura di fusione/solidificazione del materiale a cambiamento di fase fluidizzato sull'accumulo di energia termica stagionale, la massimizzazione della frazione solare e la funzionalità dell'impianto.

Nello specifico la creazione numerica di un profilo orario di domanda di energia termica per riscaldamento da associare al collettore solare in progetto è descritta nell'approfondimento 2. Il profilo orario di richiesta termica per riscaldamento è stato sviluppato per l'intera stagione invernale, per un alloggio tipo equipaggiato con pavimenti radianti e collocato nel clima di Torino. A valle della calibrazione dei risultati di simulazione, il profilo così ottenuto è stato utilizzato per valutare le necessità di accumulo termico in funzione di diversi livelli termici impostati (a seguito della selezione del materiale slurry-PCM) andando a fare un'analisi di sensibilità sulle principali variabili del sistema (numero di pannelli, temperatura di lavoro, ecc.) Sono stati altresì raccolti profili di richiesta di energia termica per riscaldamento reali da utilizzarsi nella simulazione del comportamento del collettore solare in progetto.

Con specifico riferimento ai sistemi per il controllo climatico basati su concetti mirati alla minimizzazione delle differenze di temperatura, i risultati ottenuti e presentati in questa relazione si possono schematizzare nei seguenti punti:

- individuazione del concetto di schema impiantistico su cui basare la futura sperimentazione (vi è l'intenzione di realizzare, in collaborazione con aziende del settore, un dimostratore le cui prestazioni saranno successivamente monitorate),
- Individuazione (ed acquisizione) del PCM micro incapsulato con cui realizzare lo slurry PCM (fluido di processo),
- Creazione di un profilo temporale tipo (di riferimento) della domanda termica (di riscaldamento) sulla cui base sviluppare analisi di sensibilità per il dimensionamento/ottimizzazione del sistema impiantistico
- Simulazione – di massima – del comportamento del sistema solare a slurry PCM per individuare campi termici di funzionamento dell'impianto e dimensioni dei componenti principali.

L'attività di ricerca – al momento – è focalizzata alla progettazione e realizzazione di un circuito di laboratorio in cui misurare le proprietà termofisiche dello slurry PCM che sarà successivamente utilizzato all'interno del dimostratore.

Si evidenzia che, poiché questa attività di ricerca è iniziata nel corso di questo anno, al momento non sono state ancora prodotte pubblicazioni di carattere scientifico. Si prevede di pubblicare alcuni risultati intermedi nel corso del prossimo anno

Parallelamente, è stato sviluppato uno studio rivolto all'esame delle potenzialità di applicazione dei pannelli radianti (pavimenti e soffitti) per la climatizzazione accoppiati a sistemi impiantistici operanti a temperatura moderata. Tale studio è stato condotto anche attraverso un confronto dei suddetti sistemi con sistemi di climatizzazione tradizionali, al fine di mettere in luce i possibili risparmi energetici conseguibili attraverso l'utilizzo di soluzioni a

temperatura moderata. In “Approfondimento 3” è riportato l’Abstract dell’articolo pubblicato nella rivista internazionale HVAC&R Research su tale tematica.

Le evoluzioni delle ricerche condotte sono indirizzate a mettere in luce le potenzialità applicative di nuovi sistemi integrati del sistema edificio-impianto che interagiscono con la fonte energetica solare.

Approfondimento N. 1

Analisi dei fluidi di processo e simulazione numerica di massima del sistema solare termico innovativo

In this deliverable the different slurries phase change materials that are currently on the market are presented as a function of the fusion/solidification temperature, of the heat capacity coefficient and of the other thermophysical properties. Moreover, following the seasonal thermal load profile previously determined (annex 2), a comparison between the performance of a solar system with water and one with a mixture water-slurry PCM was done.

Nel presente deliverable vengono indagate le diverse tipologie di fluidi a cambiamento di fase fluidizzati attualmente disponibili sul mercato in funzione della temperatura di fusione/solidificazione, del calore specifico e delle altre proprietà termofisiche. A seguito dell'analisi, a partire dai dati del profilo orario stagionale di potenza termica determinato nell'allegato 2, è condotto un confronto tra le prestazioni di un impianto solare funzionante ad acqua ed uno funzionante con miscela acqua-slurry-PCM.

PCM emulsions and mPCM slurries

A new technique has been proposed to use PCM materials in thermal storage systems: this technique consists of forming a two-phase mixture fluid, such as water and a phase change material, such as paraffin, resulting in a latent heat storage fluid. Inaba has classified thermal fluids, describing the main characteristics and applications. Among the latent thermal fluids, five types of fluids are mentioned: 1) ice slurries, 2) phase change material microemulsions, in which the PCM is dispersed in water through an emulsifying agent; 3) microencapsulated PCM slurries, where the PCM is microencapsulated in a polymeric capsule and dispersed in water; 4) clathrate hydrate PCM slurries, where the clathrate hydrates are composed of water molecules (host molecule) forming a weaved structure where the molecules of the other substance (guest molecule) are accommodated, constituting a special molecular structure where the heat associated with the chemical reaction of formation and dissociation of clathrate hydrate is greater than that of ice melting; 5) shape-stabilized PCM slurries (ssPCM slurries), this consist of paraffin unfilled in high density polyethylene, with a melting temperature higher than of the paraffin. In this way the paraffin is retained inside the high density structure polyethylene, avoiding the leak of the PCM. Different types of PCM slurries: (*the case of clathrate hydrate PCM slurries does not appear drawn, In 2010 Zhang et al. published a review about thermal properties and applications).

As main issues to be tackled, some studies inform that in the case of mPCM slurries it is particularly difficult to maintain a stable homogeneous flow if the particles are not processed with very small size and high flexibility.

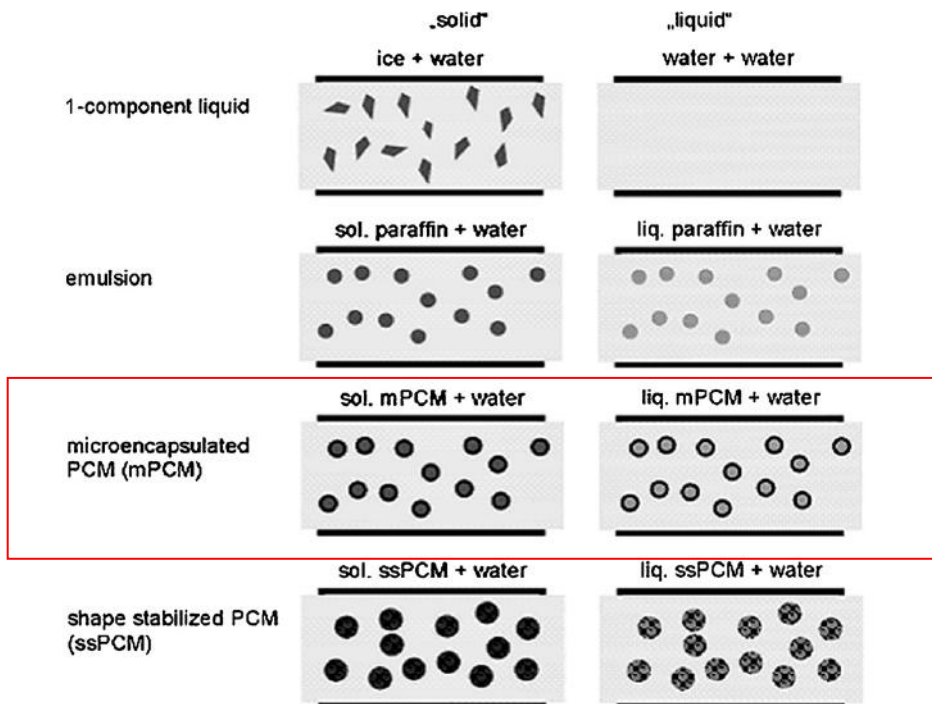


Fig.1. Schematic drawing of the different types of PCM slurries

Besides the PCM capsules entails an extra cost, the capsule prevents the PCM in continuous phase from leaking, which in that case could solidify in ducts and cause clogging. It is important that the capsules are sufficiently resistant against the stress produced by pumps. In the case of emulsions, instabilities could appear during phase change and that is difficult to maintain a stable emulsion above melting temperature. Stratification problems will appear as the paraffin droplets will form greater droplets and finally a PCM layer will float in the upper part of the storage system, due to the difference of densities.

Advantages of these new fluids as thermal storage materials or heaters transfer fluids:

- 1) High storage capacity during phase change
- 2) Possibility to use the same medium either to transport or store energy (as these slurries are pumpable), reducing in this way heat transfer losses.
- 3) Heat transfer at an approximately constant temperature.
- 4) High heat transfer rate due to higher heat capacity.
- 5) A better cooling performance than conventional heat transfer fluids, due to the decrease in fluid temperature as a consequence of higher heat capacity.
- 6) A better thermal energy storage density in comparison to conventional systems of sensible heat storage in water and can be competitive against macroencapsulated PCM tanks.

In order to be advantageous these latent fluids must meet the following requirements:

- 1) High heat capacity
- 2) Phase change temperature range matching the application.

- 3) Low subcooling
- 4) High heat transfer rate
- 5) Pumpable, low pressure drop in pumps systems
- 6) Stable over a long term storage
- 7) Stable at thermal-mechanical loads in pump systems.

Fabrication of PCM microcapsules

Microencapsulation: in recent years this technique widely used in the pharmaceutical and chemical engineering fields, has reached the field of phase change materials in order to improve their behavior. The most utilized techniques for PCM microencapsulation are: the spraydrying technique, coacervation, in situ, interfacial polymerization. (*These three methods are explained on the article ‘Review on phase change material emulsions and microencapsulated phase change material slurries: Materials, heat transfer studies and

Microencapsulation Process	Core Material	Shell Material	Melting Temperature (°C)	Phase change entalpy (kJ/kg)
In situ polymerization	Tetradecane	PS (poliestirene)	2,06	0
In situ polymerization	Tetradecane	PMMA (Polymethyl methacrylate)	5,97	66,26
In situ polymerization	Tetradecane	Polyethyl methacrylate	5,68	80,62
Interfacial polymerization	n-Octadecane	Melamine formaldehyde	24	-
In situ polymerization	Paraffin	Ura-formaldehyde	54	157,5
Polymerization of emulsion	Docasane	PMMA (Polymethyl methacrylate)	41	54,6
In situ polymerization	n-Octadecane	Melamine formaldehyde	30,5	170
Polymerization	n-Octacosane	PMMA (Polymethyl methacrylate)	50,6	86,4
Coacervation/Spray-drying	Paraffin wax (Merck)	-	-	145/240
In situ polymerization	n-Octadecane	Melamine formaldehyde	40,6	144
Coacervation	n-Octadecane	-	24-29	147,1

applications’)

PCM microcapsules and mPCM slurries studied in literature

PCM	Emulsifying method	Surfactant	Melting Temperature (°C)	Phase change entalpy (kJ/kg)
Mixture of n-alkanes	Ultrasonic generator	Non-ionic surfactant	9,5	78,9
20% Tetradecane	Phase inversion	6% surfactant (67,7%Tween60 and 32,3%Span60)	-	43
Tetradecane			(10%) 5,06	(10%) 18,5
			(20%) 5,84	(20%) 112,3
			(30%) 5,84	(30%) 150,8
Mixture of hexadecane and tetradecane 70/30 and 2,5% paraffin as nucleation agent	1,5% alcohol ethoxylate			(30%RT6) 75
				(30%RT10) 50
				(30%RT20) 44
Paraffin RT10	Phase incursion		4 - 11,5	55

These two tables show only some of the PCM studied materials with their properties and the obtaining methods, extracted of the article 'Review on phase change material emulsions and microencapsulated phase change material slurries: Materials, heat transfer studies and applications' where others are also shown.

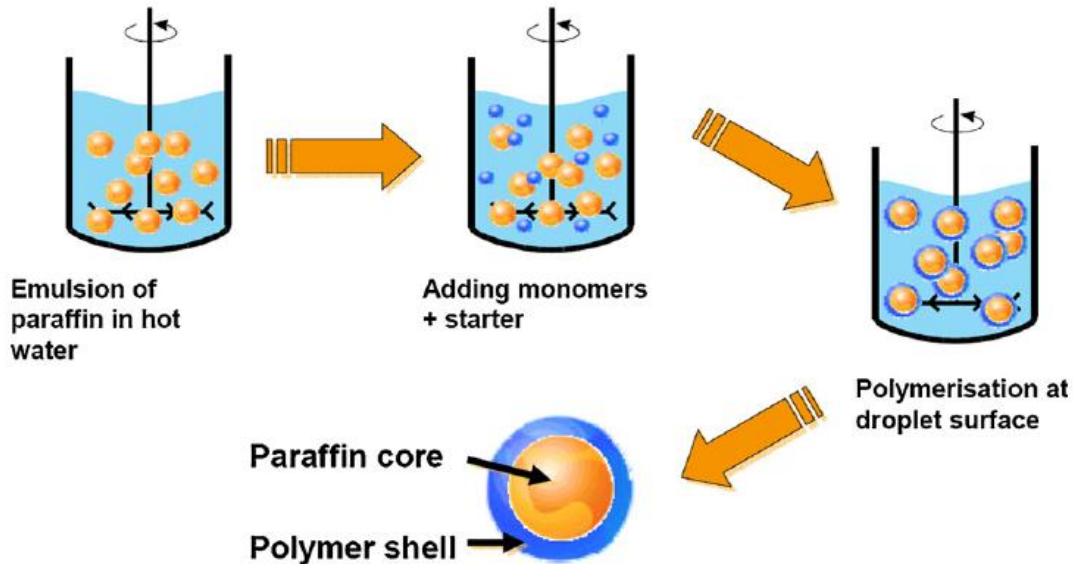


Fig.2. Microencapsulation process

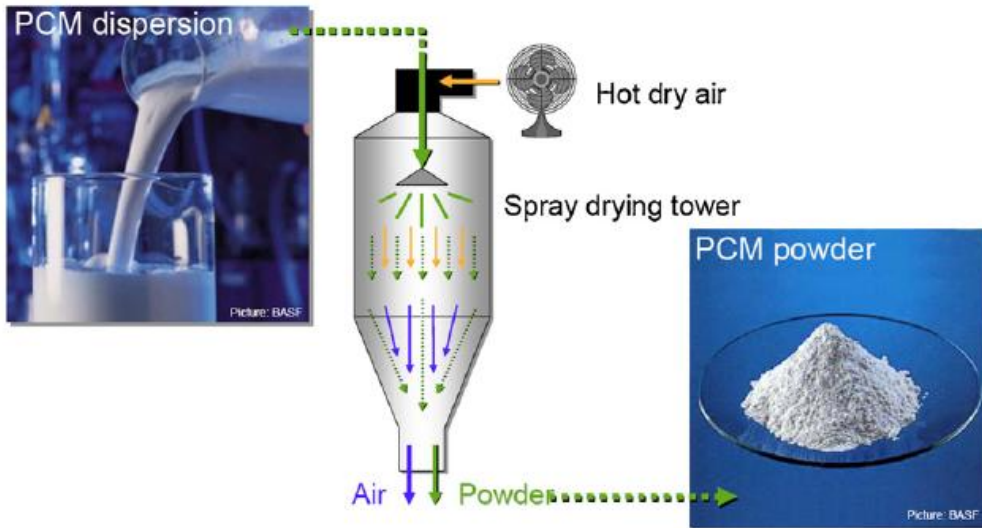


Fig.3. Drying Process

Manufacturer	Product	Type of product	PCM	Concentration	Particle/droplet size	Melting temperature	Latent heat
BASF	DS 5000	mPCM slurry	Paraffin	42%		26 °C	45 kJ/kg
	DS 5007	mPCM slurry	Paraffin	42%		23 °C	41 kJ/kg
	DS 5030	mPCM slurry	Paraffin	42%		21 °C	37 kJ/kg
	DS 5001	Powder	Paraffin			26 °C	110 kJ/kg
	DS 5008	Powder	Paraffin			23 °C	100 kJ/kg
	DS 5030	Powder	Paraffin			21 °C	90 kJ/kg
Microtek Laboratories	MPCM-30D	Powder	n-Decane		17–20 μm	–30 °C	140–150 kJ/kg
	MPCM-10D	Powder	n-Dodecane		17–20 μm	–9.5 °C	150–160 kJ/kg
	MPCM 6D	Powder	n-Tetradecane		17–20 μm	6 °C	157–167 kJ/kg
	MPCM 18D	Powder	n-Hexadecane		17–20 μm	18 °C	163–173 kJ/kg
	MPCM 28D	Powder	n-Octadecane		17–20 μm	28 °C	180–195 kJ/kg
	MPCM 37D	Powder	n-Eicosane		17–20 μm	37 °C	190–200 kJ/kg
	MPCM 43D	Powder	Paraffin mixture		17–20 μm	43 °C	100–110 kJ/kg
	MPCM 52D	Powder	Paraffin mixture		17–20 μm	52 °C	120–130 kJ/kg
Capzo	Thermusol HD35SE	Powder	Salt hydrate			30–40 °C	200 kJ/kg
	Thermusol HD60SE	Powder	Salt hydrate			50–60 °C	160 kJ/kg

- Creaming or sedimentation
- Flocculation
- Coalescence
- Ostwald ripening
- Phase inversion
- Instabilities problems (**mPCM slurries**) due to:
 - Microcapsule rupture (*Yamagishi studied the damage produced by the stress caused by the pump or by agitation on microcapsules.
 - Creaming or sedimentation

Viscosity values. PCM emulsions and mPCM slurries studies in literature

A) Dispersion system

	PCM	Weight concentration	Viscosity
	Mixture of n-alkanes	50%	25 mPa s (7 °C, stress= 3 Pa)
PCM emulsion	Tetradecane	10%	1.25 mPa s (35 °C)
		20%	2.33 mPa s (38 °C)
		30%	2.95 mPa s (38 °C)
	l-Bromohexadecane	5%	2.05 mPa s (10 °C)
			1.54 mPa s (20 °C)
		10%	2.23 mPa s (10 °C)
			1.81 mPa s (20 °C)
mPCM slurry	Tetradecane	15.80%	4.18 mPa s (10 °C)
			3.32 mPa s (20 °C)
			Newtonian behavior starting at 600 1/s
		5%	0.98 mPa s (25 °C)
			2.74 mPa s (5 °C)
		10%	1.04 mPa s (25 °C)
			1.85 mPa s (5 °C)
		15%	1.54 mPa s (25 °C)
			1.57 mPa s (5 °C)
		20%	1.94 mPa s (25 °C)
	1.39 mPa s (5 °C)		
	25%	3.31 mPa s (25 °C)	
	30%	5.23 mPa s (5 °C)	
	40%	4.21 mPa s (25 °C)	
	35%	5.53 mPa s (5 °C)	
	40%	4.11 mPa s (25 °C)	
		5.84 mPa s (5 °C)	
		12.58 mPa s (25 °C)	
		20.87 mPa s (5 °C)	

B) Water

n-Octadecane	5%	1.27 mPa s
	10%	2.3 mPa s
	20%	4.9 mPa s
		1.307 mPa s (10 °C)
		1.002 mPa s (20 °C)
		0.798 mPa s (30 °C)

Thermal properties. Thermal conductivity

The low thermal conductivity is one of the main disadvantages of thermal energy storage systems with PCMs. Some values are shown in the next table:

	PCM	Weight concentration	Thermal conductivity (W/(mK))
mPCM slurry	n-Octadecane	5%	0.571 (a 20 °C)
		10%	0.541 (a 20 °C)
		20%	0.483 (at 20 °C)
	l-Bromohexadecane	5%	0.568 (at 20 °C)
		10%	0.539 (at 20 °C)
		15.80%	0.506 (at 20 °C)
20.40%		0.48 (at 20 °C)	
	n-Eicosane	27.60%	0.446 (at 20 °C)
		5% (with 10% alumina nanoparticles)	0.66 (at 30 °C)
		10% (with 10% alumina nanoparticles)	0.62 (at 30 °C)
Agua			0.60 (a 20 °C)
			0.61 (a 30 °C)

The low thermal conductivity results in slow charging and discharging. Are numerous studies aimed at the improvement of the thermal conductivity of the PCM. The way to do that could be by embedding structures of materials with high thermal conductivity or by using finned heat exchangers or encapsulating the PCM in containers with a high surface/volume ratio. This is the reason why PCM microcapsules are interesting. Due to the microscopic size of the PCM microcapsules or droplets, the PCM slurry can be treated as a homogeneous material. This assumption implies in that the temperature gradients inside the solid are negligible. This is accomplished if the convective thermal resistance inside the microcapsules is low in comparison the convective thermal resistance between the microcapsule and surroundings.

PCM slurries in water can improve heat transfer as a consequence of the relationship area/volume of droplets in the case of emulsions and of microcapsules in the case of slurries, in comparison to systems in which the PCM is macroencapsulated. Besides, the fact of dispersing phase change particles into a fluid can improve heat transfer through convection with respect to water. These slurries can serve either as thermal storage materials or heat transfer fluids. The thermal properties of these slurries are different from those of PCM and the fluid in question, which are essential to evaluate the fluid and the heat transfer characteristics of a system with these slurries. The thermal properties to be discussed are thermal conductivity and convection heat transfer coefficient. The analysis of the different studies regarding the convection heat transfer coefficient is presented in a separate section, due to their extension and importance within this review.

Kasza and Chen studied and documented the benefits of the use of PCM slurries in water, such as the improvement in heat transfer and increase in storage efficiency. Some of the benefits mentioned are:

- 1) Reduction in the temperature difference between source and drain
- 2) Increase of heat capacity of the fluid, as a consequence of the PCM dispersion. This gives place to a lower mass flow and therefore an a lower pumping consumption.
- 3) Dynamic use of the PCM. In a conventional system, heat exchange between PCM (static use) and a separated heat transfer fluid is need to transport heat or cooling.

With PCM slurries, thermal storage and the heat transfer fluid are integrated into the PCM slurry.

Improvement in heat transfer occurs in slurries, with or without phase change. This improvement is substantially greater when considering PCM slurries.

Compilation of studies carried out on the heat transfer phenomenon in PCM emulsions and mPCM slurries

PCM emulsions

Flow regime	Type of study	Boundary condition	Geometry	Simulation tool/Numerical formulation	Experimental validation?	Ref.
Laminar	Experimental	Constant heat flux	Circular tube	-	-	[65]
Turbulent		Constant heat flux	Circular tube	-	-	[33]
		Constant heat flux	Rectangular channels	-	-	[34]
	Numerical	Constant heat flux	Circular tube	Finite differences, 2D	Ahuja [76]. Experimental validation without phase change. Differences not quantified.	[59]
		Constant heat flux	Circular tube	Finite differences, 2D	Goel et al. [74]. Differences of 34%.	[66]
		Constant heat flux	Circular tube	Fortran 90, Finite differences, 1D	Roy and Avanic [67]. Very small differences.	[67]
Laminar		Constant heat flux	Circular tube	Finite differences, 2D	Goel et al. [74]. Differences under 6%.	[68]
		Constant heat flux	Circular tube	Finite differences, 2D	Goel et al. [74]. Numerical results adjusted well to experimental results.	[69]

PCM slurries

		Constant heat flux	Circular tube	Finite differences. 2D	Goel et al. [74]. Good adjust between experimental and numerical results, and sensible to entry temperature.	[70]
		Constant wall temp	Circular tube	Finite differences. 2D	No. All available experimental results were limited to constant heat flux conditions.	[71]
		Constant heat flux	Rectangular channels	Fluent 6.2. 3D	Goel et al. [74]. Adapted the geometry of their model. The numerical results adapted well to the experimental results.	[72]
		Constant heat flux	Circular tube	Finite differences. 2D	Zeng et al. [57]. Differences under 9.4%.	[57]
		Constant heat flux	Rectangular channels	Comsol. Finite elements. 3D	Goel et al. [74]. Adapted the geometry of their model. The numerical results adapted well to the experimental results.	[73]
Turbulent	Experimental	Constant heat flux	Circular tube	-	-	[74]
		Constant heat flux	Rectangular channels	-	-	[29]
		Constant heat flux	Circular tube	-	-	[55]
	Numerical	Constant heat flux	Circular tube	Finite differences. 2D	Choi [77] Differences around 10-20%.	[75]
		Constant wall temp	Circular tube	Mathematica. Finite differences. 1D	Validation with analytical solution without phase change.	[6]
	Experimental	Constant heat flux	Circular tube	-	-	[28]

Objectives magnitudes and influential parameters at the time or selection of a PCM emulsion or mPCM slurry as heat transfer fluid or thermal storage material.

Influential factors or parameters	Objective magnitudes	Influence when the factor increases	
		Positive influence	Negative influence
Particle diameter	Rupture of microcapsules		Rupture pressure of microcapsules decreases, higher number of ruptured capsules.
	Subcooling	Greater probability of existing nucleation agents, and therefore lower subcooling.	
	Apparent hysteresis		Possible non-equilibrium between PCM and water temperatures, possibility of hysteresis
PCM concentration	Heat transfer	Improvement in convection coefficient.	
	Stability of emulsions		Creaming speed increases
	Heat capacity	Increase in heat capacity, increase in transported heat.	
	Pressure drop		Increase of viscosity, increase of pressure loss and pumping work. Up to PCM concentrations of 15-20% the increase is slightly superior to water.
	Heat transfer	Decrease in Stefan number and therefore improvement of convection coefficient.	Increase in viscosity, decrease in turbulence degree, and therefore worsening of convection coefficient.
Operation temperature range	Heat transfer	The operation temperature range must fit with the phase change temperature range, and be the narrowest possible.	Decrease of thermal conductivity, occasioning deterioration in heat transfer.

Applications

The main application present in literature is the utilization of PCM emulsions and mPCM slurries and thermal storage materials and heat transfer fluids in chilled ceilings.

-Wang and Niu presented the results of a mathematical simulation of a combined system of chilled ceiling and storage tank with a mPCM slurry, in addition to an air treatment unit for the ventilation necessities, in a room with the climatology of Hong Kong. During working hours, the mPCM

slurry flowed from the tank to the chilled ceiling, melting the PCM and releasing the latent heat. The combination of the chilled ceiling plus storage tank against a conventional water system achieved peak shaving, and therefore a smaller cooling unit/chiller could be sufficient. The consumptions were practically the same for the mPCM slurry and water. Nevertheless, it

must be taken into account that calculations were carried out using the same COP for the case of the tank with water and mPCM slurry, when in reality the COP for the case of the tank with mPCM slurry is higher due to operation at lower environment temperatures (charging during the night).

-Griffiths and Eames studied experimentally the pumping of a mPCM slurry from BASF manufacturer through a chilled ceiling in a room. The room was tested during four months with a 40% PCM concentration. When water was pumped through the chilled ceiling, a mass flow of 0.7 l/s was required for an inlet temperature of 16 °C and outlet temperature of 18 °C, maintaining the room at 19 °C. When water was substituted by the mPCM slurry, the slurry was capable of maintaining a temperature of 20–21 °C with a mass flow of 0.25 l/s. This means that the ceiling required a lower mass flow (pumping savings were not quantified), could absorb energy at a constant temperature, avoiding increments in the panel surface temperature when internal gains increased.

-Another well-known application, similar to the previously described, was carried out at the Narita Airport in Tokio by Shibutani. The issue in the installation of the Narita Airport in Tokio was the change of refrigerants due to environmental reasons. When R11 and R22 were substituted by R134a and R123 without changing the chiller unit, this resulted in lower cooling power and the chiller was non-capable to absorb the demand peaks at specific times of the day. This problem was solved through the installation of a tank filled with a mPCM slurry custom-developed by Mitsubishi Heavy Industries. The characteristic temperatures on the demand side were a supply temperature of 5 °C and a return flow temperature of 12 °C. A mPCM slurry was selected with a phase change temperature range between 5 and 8 °C. The demand peaks occurred between 8:00 and 22:00, and therefore the cooling produced during the night by the chiller unit could be stored and reduce the demand peaks during the day. The slurry presented a storage density of 67 MJ/m³, lower in comparison to an ice tank, 167 MJ/m³, but higher in comparison to water, 21 MJ/m³. Both the COP of the system and the operational costs for water and mPCM slurry were similar and lower than the ice tank.

References:

- Royon L, Guiffant G. Forced convection heat transfer with slurry of phase change material in circular ducts: A phenomenological approach. *Energy Convers Manage* 2008;49:928–32.
- Alvarado JL, Marsh C, Sohn C, Phetteplace G, Newell T. Thermal performance of microencapsulated phase change material slurry in turbulent flow under constant heat flux. *Int J Heat Mass Transfer* 2007;50:1938–52.
- Rao Y, Dammel F, Stephan P, Lin G. Convective heat transfer characteristics of microencapsulated phase change material suspensions in minichannels. *Heat Mass Transfer* 2007;44:175–86.
- Choi E, Cho YI, Lorsch HG. Forced convection heat transfer with phase-change-material slurries: turbulent flow in a circular tube. *Int J Heat Mass Transfer* 1994;37:207–15.
- Choi M, Cho K. Effect of the aspect ratio of rectangular channels on the heat transfer and hydrodynamics of paraffin slurry flow. *Int J Heat Mass Transfer* 2001;44:55–61.
- Griffiths PW, Eames PC. Performance of chilled ceiling panels using phase change material slurries as the heat transport medium. *Appl Therm Eng* 2007;27:1756–60.
- Wang X, Niu J, Li Y, Wang X, Chen B, Zeng R, et al. Flow and heat transfer behaviors of phase change material slurries in a horizontal circular tube. *Int J Heat Mass Transfer* 2007;50:2480–91.
- Zeng R, Wang X, Chen B, Zhang Y, Niu J, Wang X, et al. Heat transfer characteristics of microencapsulated phase change material slurry in laminar flow under constant heat flux. *Appl Energy* 2009;86:2661–70.

Charunyakorn P, Sengupta S, Roy SK. Forced convection heat transfer in microencapsulated phase change material slurries: flow in circular ducts. *Int J Heat Mass Transfer* 1991;34:819–33.

Kasza KE, Chen MM. Improvement of the performance of solar energy or waste heat utilization systems by using phase-change slurry as an enhanced heat-transfer storage fluid. *J Sol Energy Eng* 1985;107:229–36.

Roy SK, Avanic BL. Laminar forced convection heat transfer with phase change material emulsions. *Int Commun Heat Mass Transfer* 1997;24:653–62.

Zhang Y, Faghri A. Analysis of forced convection heat transfer in microencapsulated phase change material suspensions. *J Thermophys Heat Transfer* 1995;9:727–32.

Roy SK, Avanic BL. Laminar forced convection heat transfer with phase change material suspensions. *Int Commun Heat Mass Transfer* 2001;28:895–904.

Hu X, Zhang Y. Novel insight and numerical analysis of convective heat transfer enhancement with microencapsulated phase change material slurries: laminar flow in a circular tube with constant heat flux. *Int J Heat Mass Transfer* 2002;45:3163–72.

Lu W, Bai F. A new model for analyzing laminar forced convective enhanced heat transfer in latent functionally thermal fluid. *Chin Sci Bull* 2004;49:1457–63.

Xing QQ, Tao YX, Hao YL. Performance evaluation of liquid flow with PCM particles in microchannels. *ASME J Heat Transfer* 2005;127:931–40.

Zhao Z, Hao R, Shi Y. Parametric analysis of enhanced heat transfer for laminar flow of microencapsulated phase change suspension in a circular tube with constant wall temperature. *Heat Transfer Eng* 2008;29:97–106.

Sabbah R, Farid MM, Al-Hallaj S. Micro-channel heat sink with slurry of water with micro-encapsulated phase change material: 3D-numerical study. *Appl Therm Eng* 2009;29:445–54.

Kuravi S, Kota KM, Du J, Chow LC. Numerical Investigation of flow and heat transfer performance of nano-encapsulated phase change material slurry in microchannels. *J Heat Transfer: Trans ASME* 2009;131:062901.

Goel M, Roy SK, Sengupta S. Laminar forced convection heat transfer in microcapsulated phase change material suspensions. *Int J Heat Mass Transfer* 1994;37:593–604.

Roy SK, Avanic BL. Turbulent heat transfer with phase change material suspensions. *Int J Heat Mass Transfer* 2001;44:2277–85.

Wang X, Niu J. Performance of cooled-ceiling operating with MPCM slurry. *Energy Convers Manage* 2009;50:583–91.

Shibutani S. PCM-micro Capsule Slurry Thermal Storage System for Cooling in Narita Airport. In: *Proc. of 3rd Experts meeting and Workshop of IEA Annex 17*. 2002.

The main part of the information of this report has been obtained from the paper:

‘Review on phase change material emulsions and microencapsulated change material slurries: Materials, heat transfer studies and applications’

Authors: Mónica Delgado , Ana Lázaro, Javier Mazo, Belén Zalba

Aragón Institute for Engineering Research (I3A), Thermal Engineering and Energy Systems Group, University of Zaragoza, Spain

Solar circuit simulation - Parametric Data Analysis

A parametric real time simulator has been created, leading us to simulate all the cycle performance depending on the input conditions at each interval of time. It will represent a good overview of how the circuit will perform and which are going to be the decisive variables on it.

Moreover, it will allow us to appreciate the technological feasibility of the project. Taking inputs such as the number of solar collectors and the accumulator dimensioning as a starting point, several values can be determined: the amount of demand that can be covered (solar fraction), the quantity of mixture stored at a specific time in the tank and the energy loss the system is not able to take benefit from, for example.

From here on, a reasonable decision should be made about which the optimum number of solar collectors and the accumulator volume will be. Nevertheless, the circuit system should not only be chosen to cover the maximum heating demand. It is also important to consider other aspects such as the size of the accumulator and capacity to emplace it, the quantity of

fluid or mixture needed to be stored and to flow through the circuit, the overall cost of the heating system, among others.

This simulator also shows a good approximation of how the charge and discharge of the accumulator tank will be depending on each mean hour weather conditions of the flat's placement (Torino – Italy).

Pursuing all these issues, the program created is based on some constant and modifiable inputs:

Constant inputs	Modifiable inputs
- Mean hourly outdoor dry bulb temperature (T_{∞})	- Number of solar collectors
- Mean hourly radiation received per m^2 of collector at operational inclination (G_T)	- Accumulator sizing
- Constant parameters and features of the solar collector	- Mean temperature of the mixture at the solar collector (T_m)

The mean hourly constant outputs (dry bulb temperature and radiation received on a reference collector of $1m^2$) are outputs obtained from the EnergyPlus simulation and the weather conditions introduced.

Simulation features and variables - Collector characterization

The instantaneous efficiency of the solar collector is needed to assess an estimation of the heating production at real time. It provides the basis for simulation models of thermal processes and for setting up the procedure for assessing the collector performance.

Data such as radiation received per m^2 of collector at a specific inclination (G_T), ambient temperature (T_{∞}) and wind speed are recorded and allow the characterization of a collector by parameters that indicate how the collector absorbs energy and how it loses energy to the surroundings.

The next equation for η_i is a nonlinear expression also used in “Energy balance of the flat plate solar collector” section. It was firstly formulated by *Cooper and Dunkle* (1981). In this equation the instantaneous efficiency is referred as a function of the arithmetic average of the fluid inlet and outlet temperatures (T_m) and also of the overall loss coefficient (U_l). The values of the constant parameters (η_0 , a_1 and a_2) are given by the manufacturer of the collector and were displayed before in page 14 with other features.

This method is the basis of standard EU collector efficiency formulation.

$$\eta_i = \eta_0 - a_1 \cdot \frac{\Delta T_{m,i}}{G_{T,i}} - a_2 \cdot \frac{\Delta T_{m,i}^2}{G_{T,i}}$$

Where, $\Delta T_{m,i}$ is the mean fluid temperature difference and it is calculated as:

$$\Delta T_{m,i} = T_m - T_{\infty,i} = \left(\frac{T_{f,i} + T_{f,0}}{2} \right) - T_{\infty,i}$$

The values of G_T corresponding to each timestep were obtained from the EnergyPlus simulation by implementing a reference surface at the operational inclination and with the same dimensions than the selected solar collector. Thus, the program exhibited the values of mean hourly radiation received per m^2 that our solar collector would have received throughout all the simulation period.

The temperature T_{∞} corresponding to each timestep was also obtained from EnergyPlus as the output “Outdoor dry-bulb temperature”.

The temperature T_m was supposed to be constant and its value depended on the flowing fluid or mixture. It represents the mean temperature that is reached in the solar collector in normal

operational conditions. Its assigned values, when the flowing fluid is water or when it is only PCM, are 55°C and 37°C, respectively.

Note: Only two study cases were simulated. The first system used water as the flowing fluid and the second system one used a fluid consisting only on the selected PCM. The second case is obviously not real, since the PCM is not able to flow by itself. Water in a good proportion is needed to ensure the correct flowing of the mixture through the circuit. However, in these first steps of the project, experimental tests to determine which would be the best density of the mixture and therefore the proportions of the water-PCM mixture to be implemented have not been developed yet. From this approach, the first hypothetical system using water represents the performance of the system as the reference one, which is already being applied nowadays. The second hypothetical case should be understood as an ideal system that only uses PCM. Thereby, the real case performance would be found in an intermediate point in between those two.

Solar collector instantaneous efficiency (η_i)

The instantaneous efficiency (η_i) was assessed as:

$$\text{If } \begin{cases} G_{T,i} > G_{T,critical} & \longrightarrow & \eta_i > 0 \\ G_{T,i} \leq G_{T,critical} & \longrightarrow & \eta_i = 0 \end{cases} \quad (\text{by Eq. of page 45})$$

Where $G_{T,critical}$ represents the value of solar radiation from which no useful energy gain can be produced. That is:

$$\left. \begin{aligned} Q_u &= \eta_i \cdot A_c \cdot (G_{T,critical})_i = 0 \\ \eta_i &= \eta_0 - a_1 \cdot \frac{\Delta T_{m,i}}{G_{T,i}} - a_2 \cdot \frac{\Delta T_{m,i}^2}{G_{T,i}} \end{aligned} \right\} (G_{T,critical})_i = \frac{a_1 \cdot \Delta T_{m,i} + a_2 \cdot \Delta T_{m,i}^2}{\eta_0}$$

Energy production (Wh)

The solar collector energy production was assessed as:

$$\text{If } \begin{cases} \eta_i > 0 & \longrightarrow & (Production)_i = \eta_i \cdot (Total\ radiation\ received)_i \\ \eta_i = 0 & \longrightarrow & (Production)_i = 0 \end{cases}$$

Where the total amount of solar radiation received was calculated as:

$$(Total\ radiation\ received)_i = N \cdot A_c \cdot G_{T,i}$$

N: Number of solar collectors used (modifiable input)

A_c : Effective collector area

Energy demand (Wh)

The energy demand was obtained for each timestep as an EnergyPlus output (Plant Loop Heating Demand (Wh)).

Accumulated energy (Wh)

The accumulated energy represents the energy that may be stored in the storage tank or accumulator for each timestep. Defining a variable X as:

$$X = [(Production)_i - (Demand)_i] + E_{accum,i-1}$$

And knowing that the initial value of accumulated energy at the starting point of the simulation is 0, the accumulated energy was assessed during the rest of the performance as:

$$\text{If } \begin{cases} X \leq 0 & \longrightarrow & E_{accum,i} = 0 \\ X > 0 & \longrightarrow & \begin{cases} \text{If } X \geq E_{max,stored} & \longrightarrow & E_{accum,i} = E_{max,stored} \\ X < E_{max,stored} & \longrightarrow & E_{accum,i} = X \end{cases} \end{cases}$$

Demand not satisfied (Wh)

The sum of the immediately previous value of energy accumulated ($E_{accum,i-1}$) and the actual energy production may supply the actual energy demand. If it does not occur, the rest of the demand which have not been supplied will be named as “not satisfied demand”. From this approach, the assessment of the not satisfied demand was:

$$\text{If } \begin{cases} X < 0 & \longrightarrow & (\text{Demand not satisfied})_i = -X \\ X \geq 0 & \longrightarrow & (\text{Demand not satisfied})_i = 0 \end{cases}$$

Loss energy (Wh)

The energy loss represents the energy that cannot be stored in the accumulator when there is too much production. It was calculated as:

$$\text{If } \begin{cases} X > E_{max,stored} & \longrightarrow & (\text{Loss energy})_i = X - E_{max,stored} \\ X \leq E_{max,stored} & \longrightarrow & (\text{Loss energy})_i = 0 \end{cases}$$

Simulation analysis and discussion

The most significant parameters are the number of solar collectors and the accumulator sizing. The number of solar collectors limits the energy production and therefore the energy accumulated, facing a constant demand. The total energy production should be, at least, equal or higher than the total energy demand. For this reason, the number of solar collectors that produces more than the 2310.09 kWh demanded throughout all the simulation period, was checked. It was found that five solar collectors were the minimum number of solar collectors needed to satisfy the total energy demand. On one hand, if any accumulator was used, only a 9.56% of the total energy demand would be supplied. On the other hand, the 60% of the total heating demand would be satisfied if a huge accumulator of 13.000 L of water was used.

In the first case, all the energy produced during one hour must be consumed in the same hour (hourly values of production, demand, accumulation and losses); if not, this energy produced becomes an energy loss. The presence of the accumulator and its dimensions properly calculated are important and relevant factors of the system performance. The accumulator should be dimensioned to cover the maximum energy demand (or solar fraction) as possible, but always satisfying restrictive parameters. For instance, these limit values could be the overall cost or the space to emplace the tanks. A commonly applied circulating fluid flow in heating systems that use water as fluid is of ca. 50 or 75 L of fluid per m² of solar collector. This value can serve as reference in the sizing of the accumulator tank.

The number of solar collectors may be also limited, either by the overall cost or by the available surface on the top of the building to emplace them. The latter issue has been studied deeply.

Assuming that a building with other apartments like the studied and a top roof building area of 130.06m², the assessment of the maximum number of solar collectors that can be emplaced there is shown in the following lines:

The minimum distance between solar collectors to avoid that one line of collectors doesn't block out the sun to the next one is:

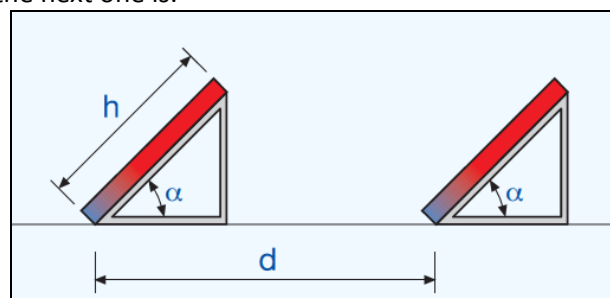


Figure 4. Sketch of the minimum distance between solar collectors
 $\alpha = 55^\circ \longrightarrow d = h \cdot 3.4 = 1.205 \cdot 3.4 = 4.097 \approx 4.1 \text{ m}$

Therefore, a hypothetical distribution could be done in an overall roof surface of $11 \times 12 \text{ m}^2$ in which 15 solar collectors can be set up:

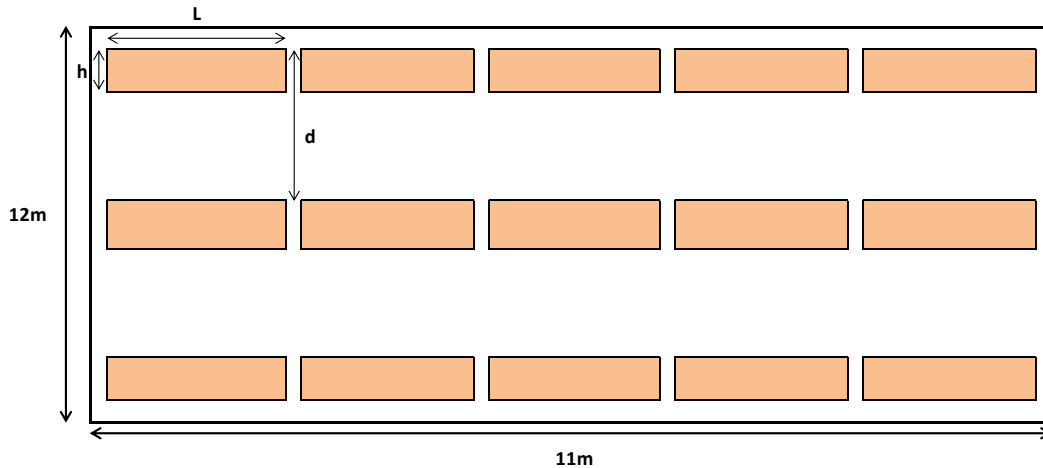


Figure 5. Sketch of a hypothetical distribution of the solar collectors

In order to decide the final number of solar collectors and the accumulator size, Fig. 6 shows the evolution of production and demand of one reference day.

Fig. 6 was developed to make a good decision about which the number of solar collectors and the volume of the storage tank would be.

- Y-axis: the solar fraction represents the energy demand supplied and it is the main reference parameter. The maximum value that it can take is 1, and it would correspond to the supply of all the heating demand.
- X-axis: number of solar collectors, from one to ten.
- Finally, each curve corresponds to a specific storage volume of the accumulator tank.

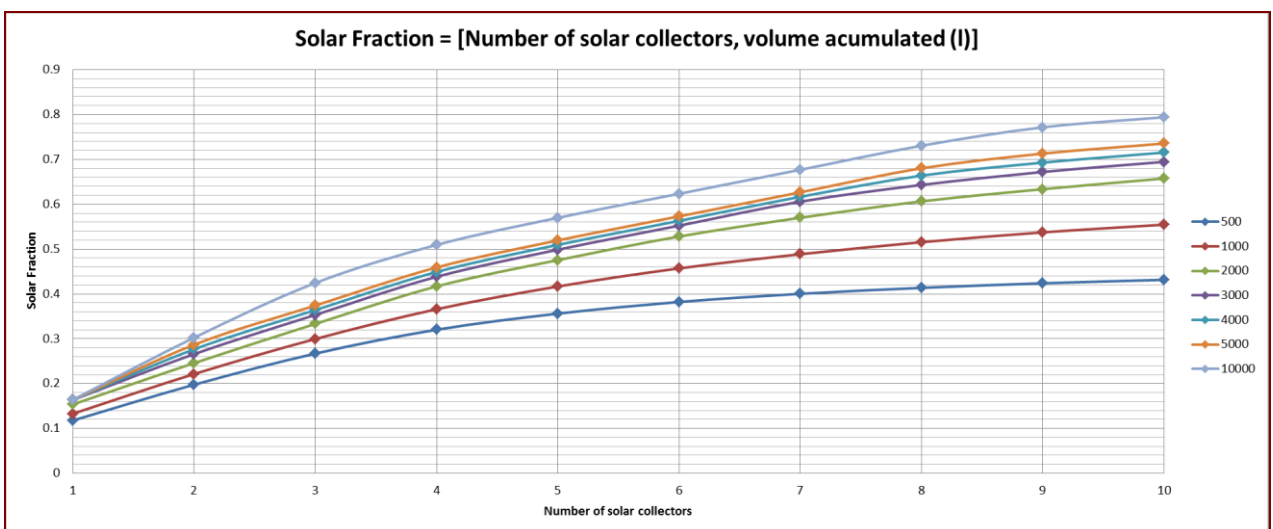


Figure 6. Plot of the solar fraction depending on the number of collectors and the tank volume.

Fig. 6 is a very useful plot since the solar fraction can be understood as function of the number of solar collectors and the accumulator volume. Typical solar fractions for water heating systems are 0.5 – 0.75. Therefore, and trying not to oversize the tank and the number of solar collectors, the system would be properly sized with 7 or 8 solar collectors and an accumulator of 4000L.

The selected volume of 4000L is equal to 93kWh of energy that can be stored during all the simulation period.

Moreover, the optimum number of collectors would be eight and the corresponding solar fraction of 0.66. On the other hand, a solar fraction of 0.62 would be covered with seven solar collectors. Assuming that the building is composed by two apartments and eight solar collectors for each apartment, the total collecting surface will be of 18.8m².

The simulation results for the selected configuration are shown in the next pages:

Selected configuration

Number of solar collectors	8
Accumulator volume (L)	4000

- The total production represents the 165% (3827kWh) of the total energy demand.
- The demand not satisfied represents the 33.6% (776.2kWh) of the total energy demand.
- Energy losses that could not be stored represent the 57.5% (2200.2kWh) of the total energy production.

Note: In future studies, the high amount of loss energy should be deeply thought as a new energy source that could be used to supply other energy demands. This energy is lost since the tank cannot store all the amount of energy produced. The stored energy is limited by the tank dimensions and the volume of fluid flowing.

Energy accumulated in the storage tank (hourly)

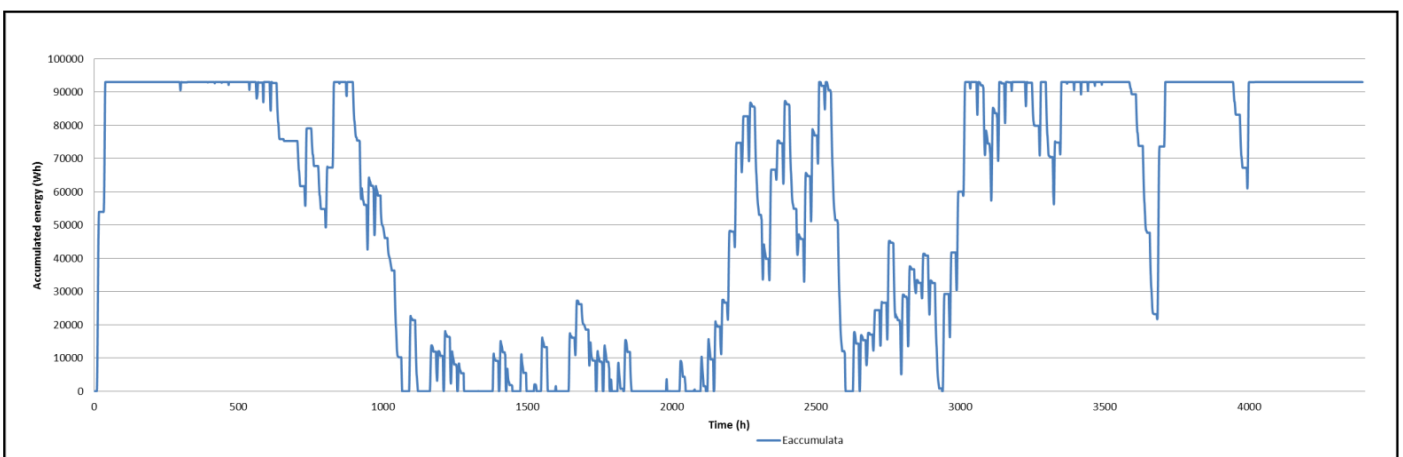


Figure7. Plot of the energy accumulated evolution

Fig. 7 displays how the energy accumulation performed at each hour during all the simulation period. It should be noted that it exhibits only the performance during the months of December, January and February, which are the coolest, and the tank cannot be filled up because of the low production and the high demand.

Demand not satisfied (hourly)

Figure 8. Plot of the demand not satisfied evolution

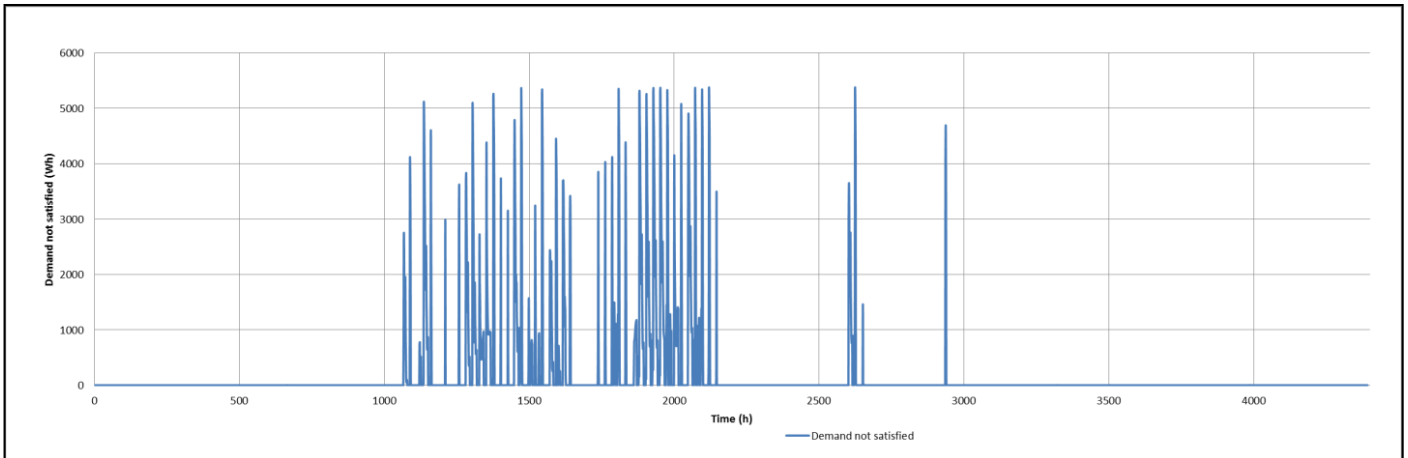


Fig. 8 displays the demand that cannot be supplied because of the low production and the dimensions of the accumulator tank. This demand, as it can be observed, is completely interrelated with the energy accumulated at each timestep. The periods with low values of energy accumulation and with high demand and low production are the periods when the largest amount of demand not satisfied is reached.

Loss energy (hourly)

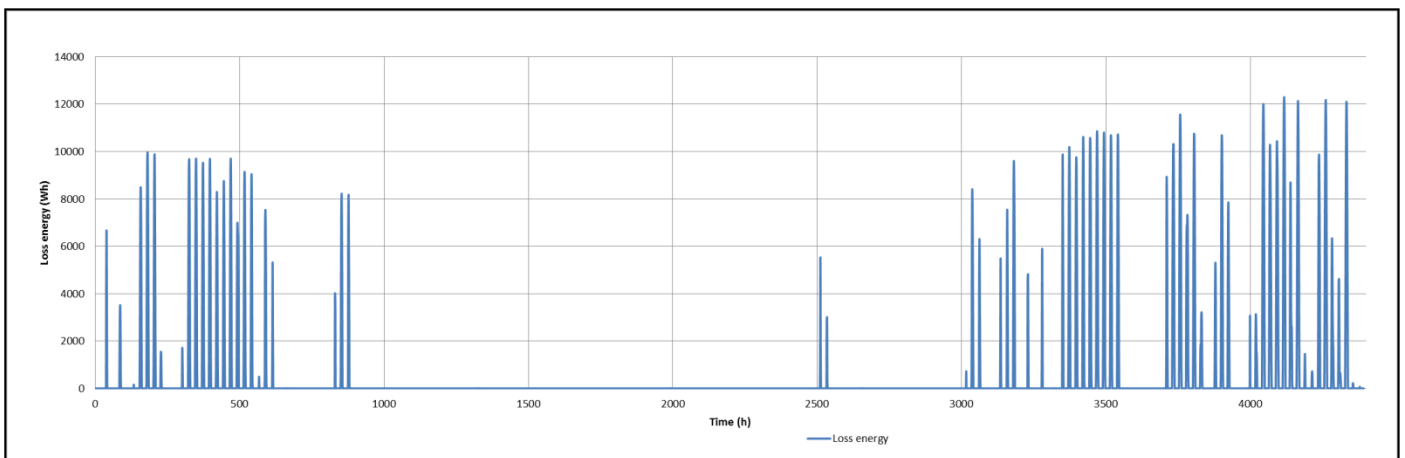


Figure 9. Plot of the energy loss evolution

Fig. 9 displays the energy that cannot be stored because of the accumulator dimension. This energy, as it was explained before, represents the largest amount of energy losses and overlaps in periods of high production. On the other hand, during the coolest months of December, January and February no energy is lost, thus all the production is consumed.

Energy variables confrontation (daily)

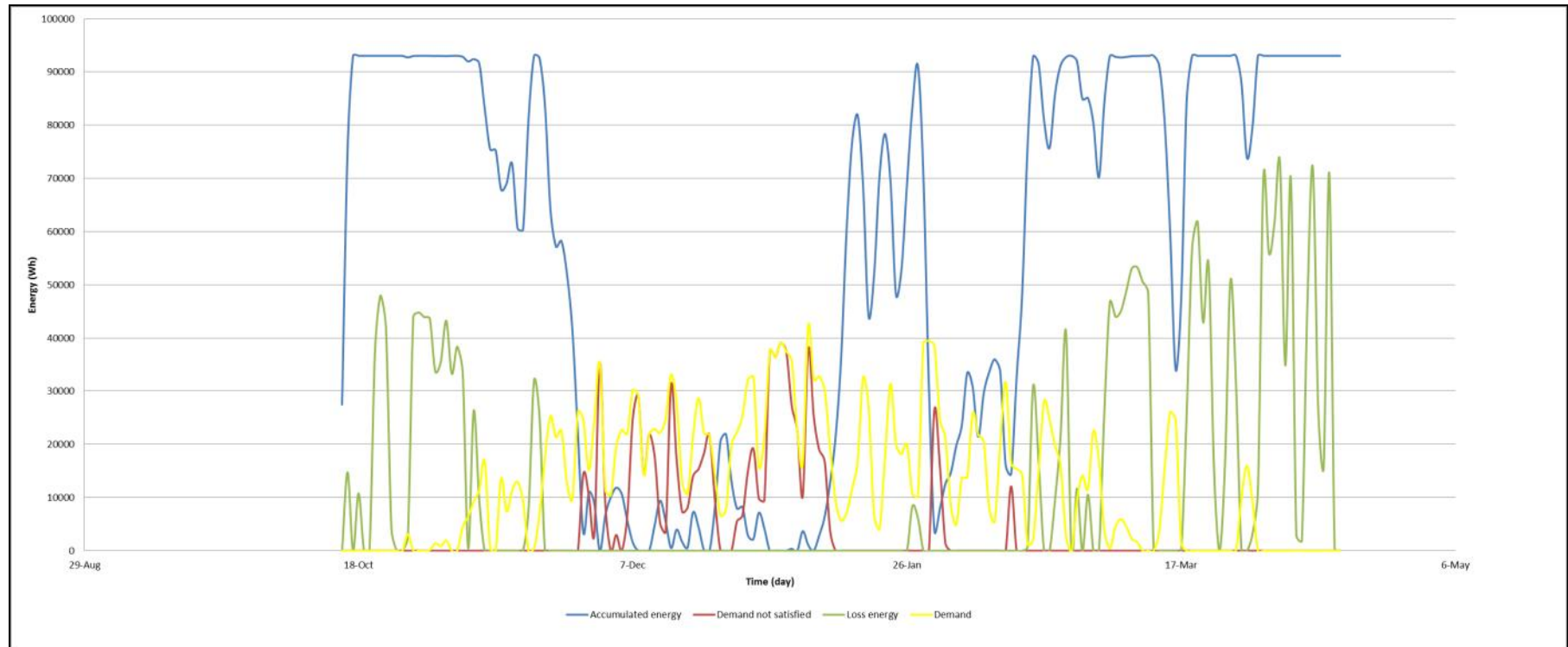


Figure 10. Plot of the main parameters daily evolution

Production vs Demand (daily)

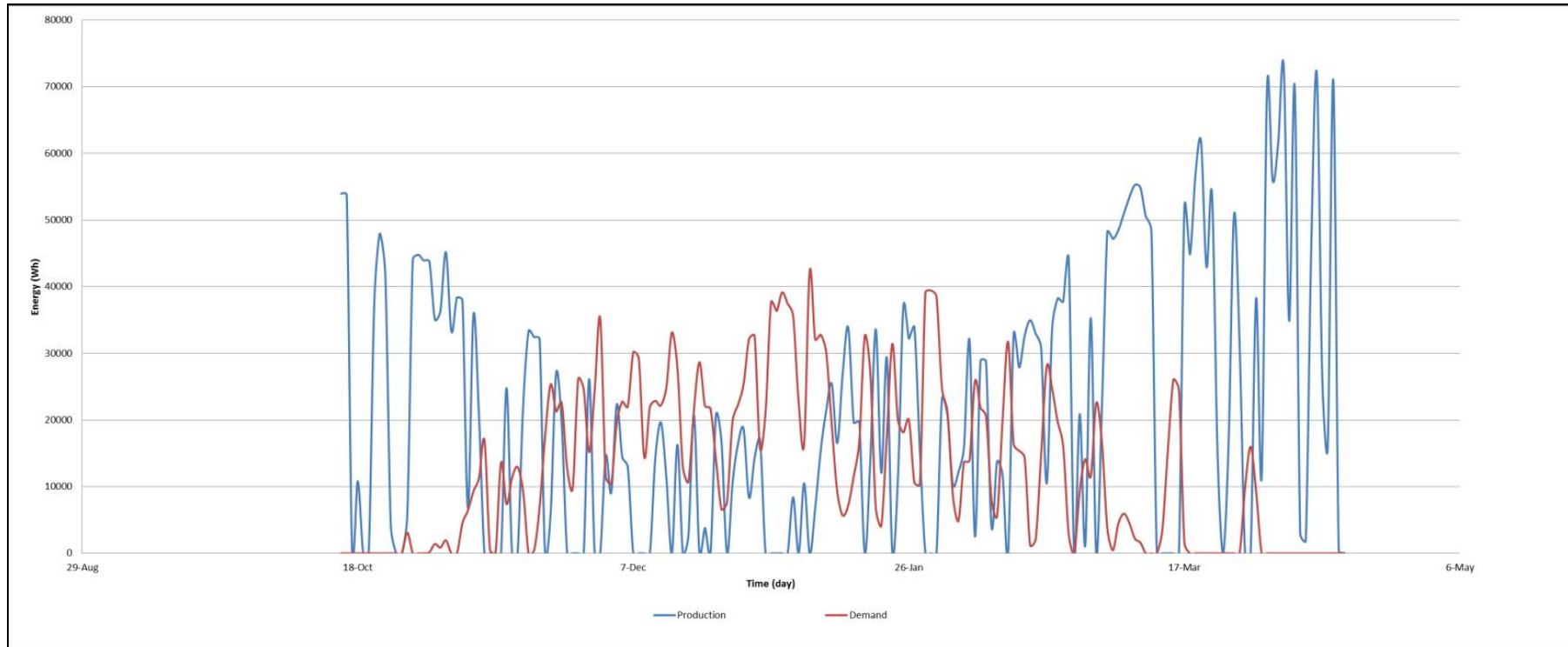


Figure 11. Plot of the production and demand daily evolution

Fig. 9 was developed in order to confront the following variables: accumulated energy, demand not satisfied, loss energy and energy demand. These have been simplified to a daily timestep instead of hourly. Therefore, every twenty four mean hourly values one average has been represented.

Fig. 10 displays the comparison of the mean daily production and the mean daily demand. It can be noted how 8th of January is the worst day of the simulation, being the demand at its highest value (42326.55W) and with no production at all. In the other hand, considering an ideal day with the largest production and energy demand is for instance, the 5th of March with an overall energy production of 48463.84W and an energy demand of 4446.51W. However, as it could be seen in the plot, it is not the most common situation.

Production vs Demand evolution during a day (hourly)

Furthermore, Fig. 12 focuses on how the production and energy demand perform during any day. The plotted day is the 25th of January, in which the production was larger than the demand.

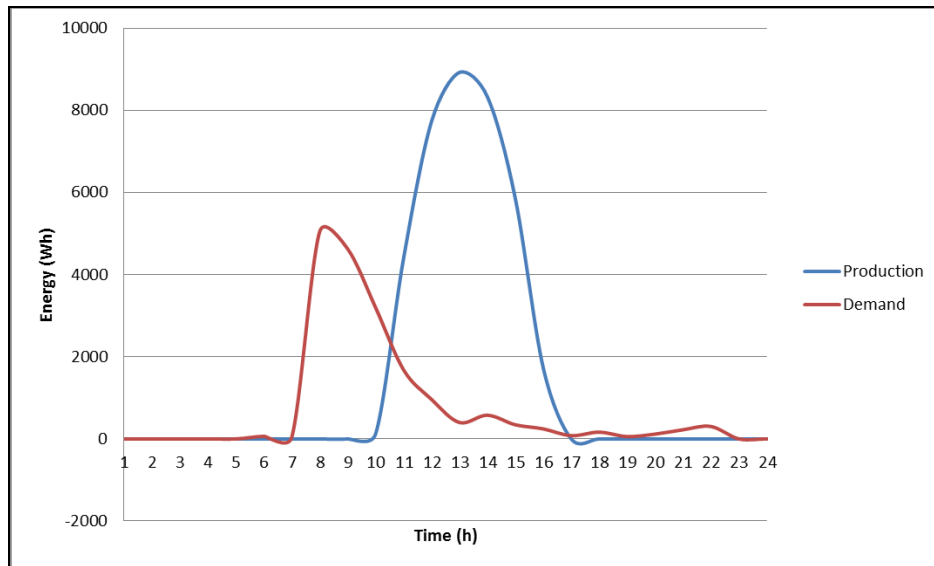


Figure 12. Plot of the production and demand evolution during one day

Analysing the daily consumption and energy requirements of a normal family it is obvious that the energy demand curve may not follow the energy production curve. It would be ideal if the red curve was always under the blue one and, from this approach, the energy could be consumed in a short time after it is produced. However, this delay in the production is the real situation and to achieve the purpose of covering the maximum energy demand it is needed to store the rest of the energy produced when there is no consume or a low one. Thereby, it is demonstrated how necessary the accumulator tank is.

Comparative study between PCM - water

All the results of the previous section have been referred to a system which only uses water. Nevertheless, as objective of the project, the system will use a mixture of water and PCM in short time. Therefore, the current section tries to present an approximated result of what it would be obtained if the fluid circulating was the PCM-water mixture, but without knowing its final proportions (% of water and % of PCM) (see page 45). However, this approximation is developed assuming that all the fluid is PCM. The number of solar collectors and the accumulator dimensions were 8 and 4000L, respectively. Some results are shown and compared to the water results in the following table.

Comparison values for water and PCM systems

	Water	PCM	% of PCM improvement from water case
Production	3827.06	5416.10	41.52
Not satisfied demand	776.22	464.54	-40.15
Accumulated energy	248810.57	293192.73	17.84
Energy loss	2200.17	3477.53	58.06

Final Conclusions

Production improvement responds to the low temperature at which the PCM works and absorbs heat in the solar collector. As it is shown in the Collector Efficiency, the collector efficiency is higher with low T_m temperatures.

Energy demand not satisfied has been reduced by a 40% compared to the water simulation. The production increase makes it possible to satisfy a larger amount of the energy demand. In an overall rate, the energy demand not satisfied in the water simulation represents the 33.6% of the total energy demand. On the other hand, the energy demand not satisfied in the PCM simulation represents the 20% of the total energy demand.

The accumulated energy increase by a 17.84% happens due to the property of the fluid to absorb more heat at a low temperature. It should be noted that the accumulator size remains the same as in the water simulation.

The energy loss increase also responds to the larger production and the limited accumulator size.

The main advantage of using a mixture of water and PCM compared to a system that only employs water as a circulating fluid is that energy can be stored in a larger amount. Therefore, the larger energy it is stored, the larger energy demand it can be satisfied. The mixture with PCM reduces the mean work temperature (T_m) and increases the solar collector efficiency. Thus much more heat will be obtained from it.

Approfondimento N. 2

Determinazione del profilo orario tipico del carico termico di riscaldamento

In this step of the project, the main objective was to determine the value of the energy demand in a specific house or apartment. To obtain that, an energy analysis and thermal load simulation program in buildings was used: *EnergyPlus*.

This software enables to model all kind of energy and mass flows as: heating, cooling, lighting, ventilation or water use. It also includes many simulation capabilities: time-steps less than an hour, modular systems and plant integrated with heat balance-based zone simulation, multizone air flow, thermal comfort, natural ventilation and photovoltaic systems.

Based on a building description, house or apartment, and on a weather file of the location, the program can calculate the heating and cooling loads necessary to maintain thermal control setpoints, the energy consumption of the primary plant equipment and the conditions throughout a secondary HVAC system and coil loads. Depth studies and continuous program improvements allowed us to think that EnergyPlus results are close to the real building ones.

EnergyPlus has been designed to be a simulation engine, an element within a system of programs that includes a graphical user interface to describe the building.

The program needs various input files that describe the building to be modelled and the environment surrounding it. The program produces several output files, which need to be described or further processed in order to make sense of the results of the simulation. The results obtained after the simulation are showed in a spreadsheet for the postprocessor results files, in a web browser for the tabular results file and in a viewer for the selected drawing file.

Input Data File

The input data file (idf) is an ASCII file containing the data describing the building and the HVAC system to be simulated. All the description of the building is included in it and all its features could be created and modified.

An apartment divided in three zones where a family of 4 people lives and with a total area of 130.06m² is going to be analysed. This flat is part of a building that has other flats like this, but our study case was simplified to one of them.

Fig. 1 shows the flat structure and its spatial situation:

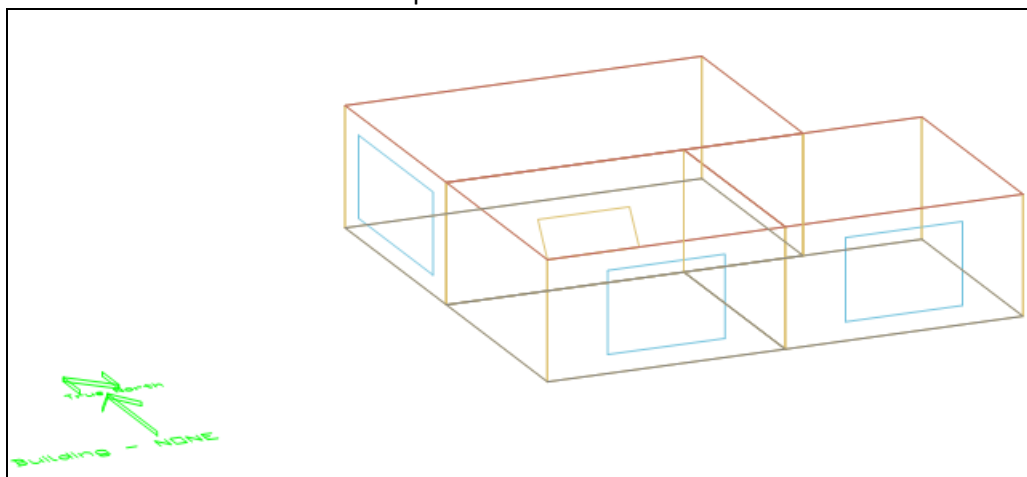


Figure 1. Sketch of the flat structure and its spatial situation

The flat has been subdivided in three zones. Each zone has a window that according to the Italian standards has a surface of at least 1/6 of the zone floor area. A solar collector of reference, with the same surface and inclination as the used one is exposed over the west zone.

The main structural features of the construction included in the input file are: dimensions, materials and construction, simulation period, weather file, internal gains and zone airflow.

Dimensions

1. Zones

Table 1. Zones dimensions

Zone	Lenght [X](m)	Widht [Y](m)	Height [Z](m)	Floor Area(m ²)
West zone	6.10	6.10	3.05	37.16
East zone	6.10	6.10	3.05	37.16
North zone	9.14	6.10	3.05	55.74
Total Area(m²)				130.06

2. Windows

Table 2. Windows dimensions

Zone	Lenght [X](m)	Widht [Y](m)	Height [Z](m)	Window Area(m ²)
West zone	3	-	2.1	6.30
East zone	3	-	2.1	6.30
North zone	-	4.5	2.07	9.32
Total Area(m²)				21.92

Materials and Construction

The elements of the building (walls, floors, roofs and windows) will determine the interactions of the building surfaces with the outside environment parameters and the internal space requirements. These surfaces are also used to represent the heat transfer through zones. To simplify the model no doors have been included.

1. External walls

The external walls are exposed to the external environment. These are composed by five layers. The materials have been chosen following one typical Italian structure.

Note: The outside layer refers to the side that is not exposed to the zone but rather the opposite side environment, which can be the outdoor environment or another zone.

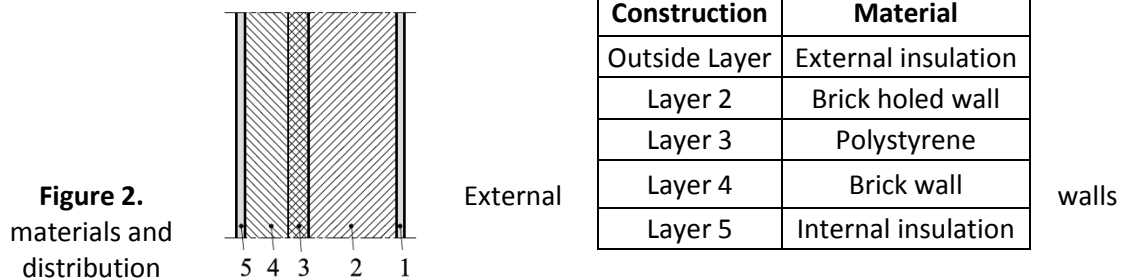


Figure 2. materials and distribution

2. Internal walls or partitions

Table 3. Internal walls materials properties

Material	Internal gypsum	Brick wall	Ins-Expanded polystyrene	Holed brick wall	External gypsum
Roughness	Smooth	Rough	Rough	Rough	Rough
Thickness(m)	0.1	0.08	5.00E-02	0.25	0.1
Conductivity(W/m·K)	0.9	0.3	3.00E-02	0.5	0.9
Density(kg/m3)	1600	725	56.06	1200	1800
Specific Heat(J/kg·K)	850	850	1210	850	850

Construction	Material
Outside Layer	G01a 19mm gypsum board
Layer 2	F04 Wall air space resistance
Layer 3	G01a 19mm gypsum board

*The Air gap filled by 'F04 Wall air space resistance' has a thermal resistance of 0.15

$$\frac{m^2 \cdot K}{W}$$

Table 4. Internal walls materials properties (II)

Material	G01a 19mm gypsum board
Roughness	MediumSmooth
Thickness(m)	0.02
Conductivity(W/m·K)	0.16
Density(kg/m3)	800
Specific Heat(J/kg·K)	1090

3. Floor and Roof

In the simulation both have been considered as adiabatic surfaces. These are common surfaces between two zones, where both zones are typically at the same temperature. Thus, no heat transfer is expected in the surface from one zone to the next, but will store heat in thermal mass. Only the inside face of the surface will exchange heat with the zone.

Table 5. Floor and roof materials and their properties

Construction: Floor	Material
Outside Layer	F16 Acoustic tile
Layer 2	F05 Ceiling air space resistance
Layer 3	M14a 100mm heavyweight concrete

Construction: Roof	Material
Outside Layer	M14a 100mm heavyweight concrete
Layer 2	F05 Ceiling air space resistance
Layer 3	F16 Acoustic tile

* The Air gap filled by 'F04 Wall air space resistance' has a thermal

resistance of $0.18 \frac{m^2 \cdot K}{W}$

Material	M14a 100mm heavyweight concrete	F16 Acoustic tile
Roughness	MediumRough	MediumSmooth
Thickness(m)	0.10	0.02
Conductivity(W/m·K)	1.95	0.06
Density(kg/m3)	2240	368
Specific Heat(J/kg·K)	900	590

4. Internal Source: Radiant Panels

The radiant panels are situated under the main floor of each zone.

Table 6. Internal sources materials and their properties

Construction: Internal Source	Material
Outside layer	Concrete - Dried sand and gravel 4 in
Layer 2	Ins-Expanded polystyrene R12 2 in
Layer 3	GYP1
Layer 4	GYP2
Layer 5	Finishing flooring - Tile 1 / 16 in

Material	Concrete - Dried sand and gravel 4 in	Ins-Expanded polystyrene R12 2 in	GYP1	GYP2	Finishing flooring - Tile 1 / 16 in
Roughness	MediumRough	Rough	MediumRough	MediumRough	Smooth
Thickness(m)	0.10	0.05	0.01	0.02	0
Conductivity(W/m·K)	1.29	0.02	0.78	0.78	0.17
Density(kg/m3)	2242.58	56.06	1842.12	1842.12	1922.21
Specific Heat(J/kg·K)	830	1210	988	988	1250

In the case of radiant systems, the construction has hydronic tubing embedded within the construction. The heat is then added to the building element to provide heating to the zone in question. The definition is similar to the Construction definition with a few additions related to radiant or other systems that will lead to source terms.

The source is present after layer number 4; therefore, it can be said that the source is located between the GYP2 layer and the Finishing flooring.

The temperature requested for the calculation is also checked after layer number 4. This allows us to calculate the temperature within the construction.

5. Windows

Table 7. Windows materials and their properties

Construction	Material
Outside Layer	LoE TINT 6MM
Layer 2	KRYPTON 8MM
Layer 3	LoE CLEAR 6MM Rev

Material: Gas	KRYPTON 8MM
Gas Type	Krypton

Thickness(m)	0.01		
Material: Glazing		LoE TINT 6MM	LoE CLEAR 6MM Rev
Optical Data Type		SpectralAverage	SpectralAverage
Thickness(m)		0.01	0.01
Solar transmittance at normal incidence		0.36	0.6
Front side solar reflectance at normal incidence		0.09	0.22
Back side solar reflectance at normal incidence		0.2	0.17
Visible transmittance at normal incidence		0.5	0.84
Front side visible reflectance at normal incidence		0.04	0.08
Back side visible reflectance at normal incidence		0.05	0.06
Infrared transmittance at normal incidence		0	0
Front Side Infrared Hemispherical Emissivity		0.84	0.1
Back Side Infrared Hemispherical Emissivity		0.1	0.84
Conductivity(W/m·K)		0.9	0.9

Simulation period

The run period selected has been from 15 of October to 15 of April, which includes the six months of heating demand by citizens of Torino (Italia).

Therefore, the total number of hours present in the simulation will be 4392.

Weather file

The weather file is an ASCII file containing the hourly or sub-hourly weather data needed by the simulation program. A data record collected during many years allows the program to iterate and confront the input and the weather files, showing output meters and spreadsheets of results.

The weather file also contains the information about the location and climate. The specific flat is situated in Torino, capital of the Piemonte region in the northwest of Italy.

The location parameters are:

Table 8. Location parameters of the flat

Location	Torino - Italy
Latitude(deg)	45.22
Longitude(deg)	7.65
Elevation(m)	287

Some of the weather parameters available and modifiable that the iteration confronts and takes into account are, among others, listed below:

- Design Conditions
- Typical/extreme periods
- Dry bulb temperature
- Dew point temperature
- Relative humidity
- Atmospheric station pressure

- Wind speed
- Wind direction
- Solar radiation (beam/diffuse)
- Sky cover

These parameters, among others, are defined in more detail at “Simulation Outputs” section.

Internal gains

Other internal sources and equipments can influence the energy consumption of the flat. People, lights, electric equipment or slab floor may come into play.

1. People

The energy gains provided by people, as well as the level of carbon dioxide generated by these are calculated and taken into account in the simulation. The flat has a family of four people. The presence of people varies as a function of the schedules, but only four people can be found as maximum: one person in the West zone, one in the east zone and two in the North zone.

The presence or non-presence of people in the flat is controlled by the schedules introduced and it is represented by a fraction. This fraction will be the same for each zone (e.g. If the fraction is 1, in the West and East zones will be one person and in the North zone will be two persons).

The schedule for the house occupancy is shown below:

- During weekdays:

Table 9. Schedule for the house occupancy

Hour Interval		Fraction occupancy
From	Until	
0:00h	6:00h	1
6:00h	7:00h	1
7:00h	8:00h	0.5
8:00h	12:00h	0
12:00h	13:00h	0.5
13:00h	16:00h	0
16:00h	17:00h	0.5
17:00h	18:00h	1
18:00h	24:00h	1

- The fraction occupancy during weekends, holidays and all other days for any time is 1
- The fraction occupancy for WinterDesignDay and holidays for any time is 1

2. Lights

The energy given by lights is another factor that must be considered as an energy gain. The lights power consumption is set in at most 5 W/m² (per zone floor area).

The house lighting is also controlled by the schedules introduced and is represented by a fraction. This fraction will be the same for each zone.

The schedule for the house lighting is shown below:

- During weekdays:

Table 10. Schedule for the house lighting

Hour Interval		Fraction lighting
From	Until	
0:00h	6:00h	0.1
6:00h	7:00h	0.2
7:00h	8:00h	0.6
8:00h	12:00h	0
12:00h	13:00h	0.5
13:00h	16:00h	0
16:00h	17:00h	0.5
17:00h	18:00h	0.6
18:00h	24:00h	0.8

- The house lighting during weekends, holidays and all other days for any time is 0.8
- The fraction lighting for WinterDesignDay and holidays for any time is 1

3. Electric equipment

The electric equipment such as television, computers, fridge and others electric appliance also contribute to the heat zone loads and therefore in increasing the mean temperature of each zone. The electric consumption is set in at most 10 W/m² (per zone floor area).

The house lighting is also controlled by the schedules introduced and it is represented by a fraction. This fraction will be the same for each zone.

The schedule for the electric equipment is shown below:

- During weekdays:

Table 11. Schedule for the electric equipment

Hour Interval		Fraction equipment
From	Until	
0:00h	6:00h	0
6:00h	7:00h	0.5
7:00h	8:00h	1
8:00h	12:00h	0
12:00h	13:00h	0.5
13:00h	16:00h	0
16:00h	17:00h	0.5
17:00h	18:00h	0.7
18:00h	24:00h	1

- The electric equipment during weekends, holidays for any time is 0.8
- The electric equipment for WinterDesignDay and holidays for any time is 1

4. Radiant panels heating system

The radiant panels are the last energy gain which contributes in the indoor temperature. It is the most significantly factor of the internal energy gain. Under each zone floor there is a radiant panel (internal source) providing heat.

The radiant panels operation is controlled by two parameters, a first “switch on” temperature that represents the minor heating water loop temperature which should be not overcome. This has been fixed with the next values for each schedule:

Table 12. Radiant panels heating system schedule

Hour Interval		Heating setpoint (°C)
From	Until	
0:00h	7:00h	18
7:00h	17:00h	21
17:00h	24:00h	18

And a second “switch off” temperature that represents the maximum heating water loop temperature which should not be overcome. This has been fixed to every hour and every day of the simulation period with a value of 35°C. The European heating standards fix the maximum value of indoor floor temperature at 29°C, so the “switch off” water value takes this into consideration.

Zone airflow

Infiltrations can be understood as a heat loss, but all the zones should be ventilated. The infiltration value is specified as a design level which is modified by a schedule fraction, temperature difference and wind speed. The calculation method has been designed as *Air Changes per hour*, being this factor:

$$\frac{\text{Air Changes}}{\text{Hour}} = 0.5$$

Simulation outputs

Each zone command generates zone outputs using the input fields above. The most common indoor and outdoor outputs are listed below:

Ambient environment outputs:

- **Outdoor Dry Bulb (°C):** The outdoor air dry-bulb temperature will be used in other sections in order to calculate the overall heat loss coefficient, losses to the environment, the solar collector efficiency and the heating production. The outdoor dry-bulb temperature will be named in other sections as “Outdoor air temperature”.

- **Outdoor Wet Bulb (°C):** The outdoor wet-bulb temperature is derived (at the timestep) from the values for dry-bulb temperature, humidity ratio and barometric pressure.
- **Outdoor Humidity Ratio (kg water/kg air):** The air humidity ratio represents the mass of water vapour to the mass of dry air. It is unit less.
- **Wind Speed (m/s):** The outdoor wind speed.
- **Wind direction (degree):** The outdoor wind direction (N=0, E=90, S=180, W=270).
- **Sky temperature (°C):** The sky temperature is derived from horizontal infrared radiation intensity. The program assess it as:

$$T_{sky} = \left(\frac{\text{Horizontal IR}}{\sigma} \right)^{\frac{1}{4}} - 273.15$$

Where $\sigma = 5.67E - 8 \frac{W}{m^2 K^4}$ (Steffan-Boltzmann constant)

- **Horizontal Infrared Radiation (W/m²):** The horizontal infrared radiation intensity is based on opaque sky cover, sky emissivity, temperature and other factors.
- **Diffuse solar radiation (W/m²):** Diffuse solar radiation is the amount of solar radiation received from the sky (excluding the solar disk) on a horizontal surface.
- **Direct (or beam) solar radiation (W/m²):** Direct solar radiation is the amount of solar radiation received within a 5.7° field of view centred on the sun. This is also known as beam solar.

Zone thermal outputs:

- **Zone Mean Air Temperature (°C):** This is the zone average temperature of the air at the timestep. The zone heat balance supposes a well stirred model for a zone; therefore, there is only one mean air temperature to represent the air temperature for the zone. It is calculated for each zone.
- **Hydronic Low Temp Radiant Heating Energy (J):** This field reports the heating input to the low temperature radiant system. This is the heat source to the surface that is defined as the radiant system. The heating rate is determined by the zone conditions, the control scheme defined in the user input, and the timestep. It is calculated for each zone.
- **Hydronic Low Temp Radiant Water Mass Flow Rate (kg/s):** This field reports the mass flow rate of water through the low temperature radiant system. It is calculated for each zone.

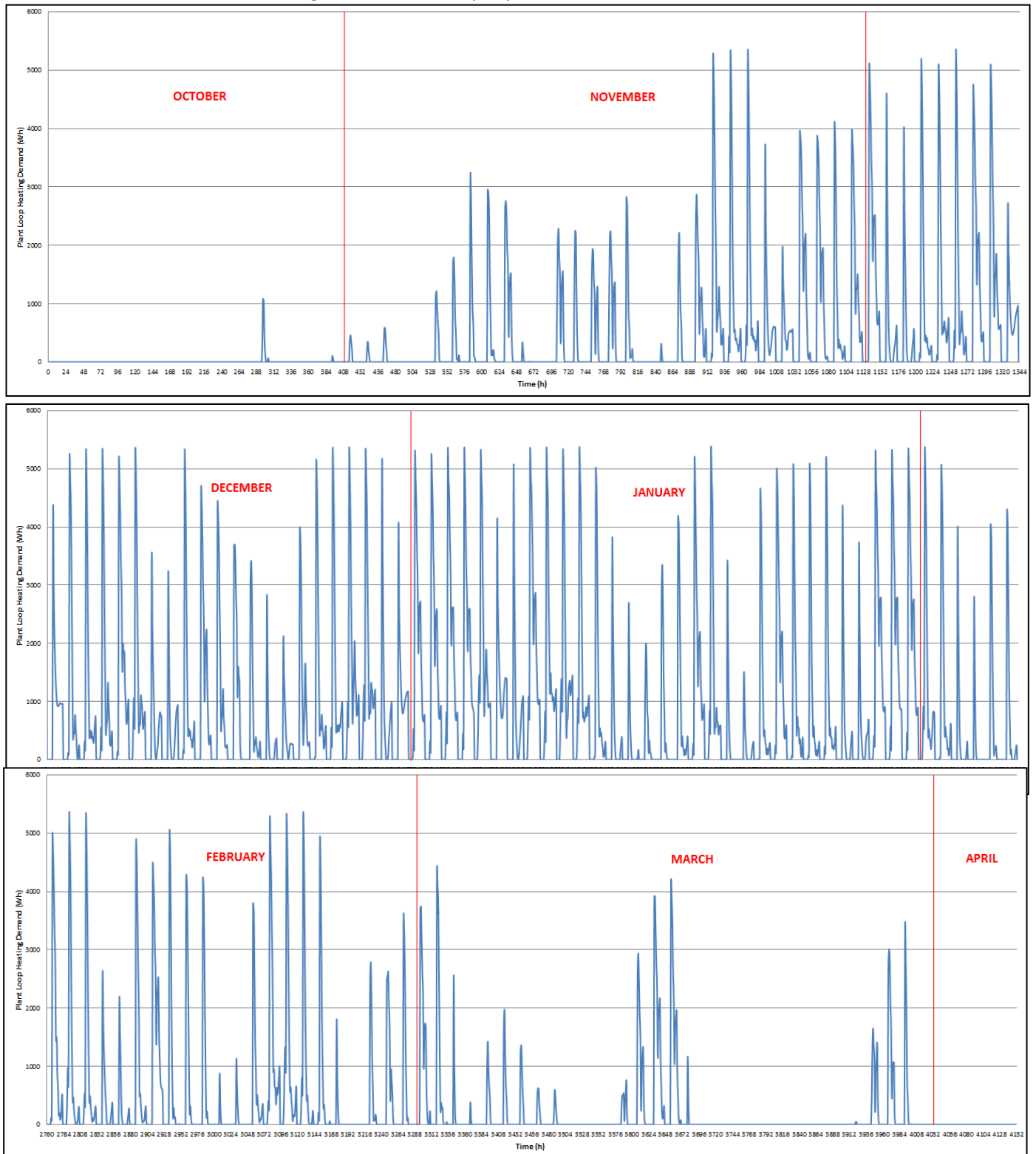
- **Hydronic Low Temp Radiant Water Mass Inlet Temp (C):** This field reports the temperature of water entering the low temperature radiant system. It is calculated for each zone.
- **Hydronic Low Temp Radiant Water Mass Outlet Temp (C):** This field reports the temperature of water leaving the low temperature radiant system. It is calculated for each zone.
- **Zone Total Internal Heat Gain (J):** These report variables represent the sum of all heat gains (radiant, convective and latent) from specific internal sources throughout the zone in watts (for rate) or joules. This includes all heat gains from: people, lights, electric equipment, gas equipment, hot water equipment and steam equipment and other equipment. It is calculated for each zone.
- **Plant Loop Heating Demand (W):** This field is not calculated for each zone, but it is the overall assessment of the heating demand of the three zones. This is the net demand required to meet the heating setpoint of the loop. In the particular case of this study, as the loop setpoint is met for the current HVAC timestep, Plant Loop Heating Demand is equal to the sum of the total heating demand from the demand side coils on the loop, that is the same value which is obtained from summing the three Hydronic Low Temp Radiant Heating Energy values (J) (one from each zone) and dividing it by 3600 (to convert J into W).

Some of the mentioned output values are plotted and analysed in the following pages in order to obtain an easy results overview.

Plant loop heating demand (hourly)

Figure 3. Plot of the plant loop heating demand along all the simulation period.

Note: There is no heating demand of the April period from 4152 to 4392 hour.



In Fig. 3 it could be appreciated how the heating demand is at first 0 and then it increases significantly at the beginnings of November. Finally, at the end of March, the heating demand also becomes 0 and there is no more demand until the ends of the simulation period.

Heating demand frequency

Fig. 4 shows the hourly frequency of the heating demand at each power rate. This and the others plots performed were referenced to the six months of simulation (from 15th of October to 15th of April):

Table 13. Percentage of hours front the total of heating demand

Heating Demand (Wh)	Percentage of total hours (%)
= 0	61.36
0 < HD ≤ 1000	22.36
1000 < HD ≤ 2000	6.67
2000 < HD ≤ 3000	3.85
3000 < HD ≤ 4000	2.37
4000 < HD ≤ 5000	2.39
≥ 5000	1

The total number of hours that were considered by the simulation period was 4392 hours. Table 17 shows how the circuit will perform only a 38.64% of the time because there is no heating demand during a 61.36% of the period.

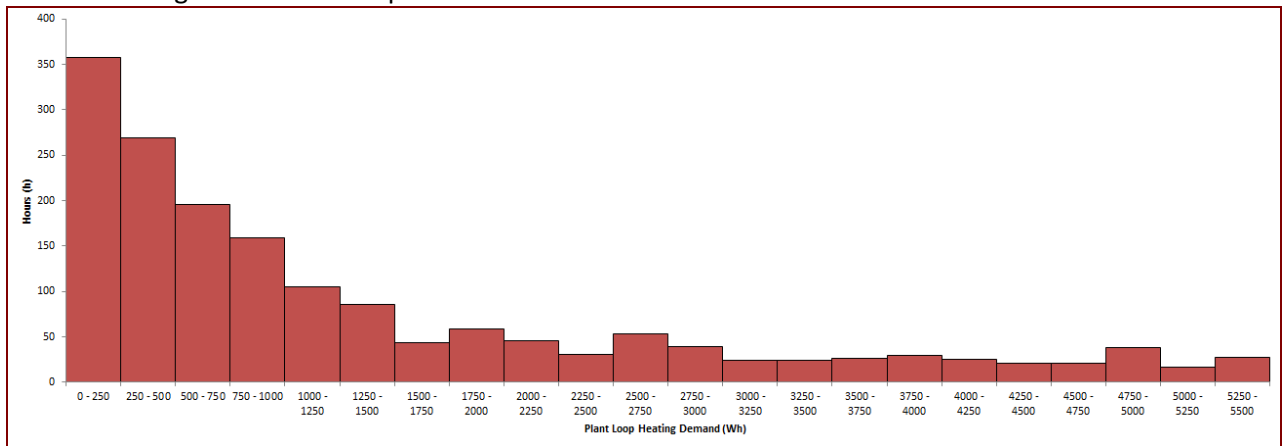


Figure 4. Plot of the total hours at each range of heating demand, when there is heating demand > 0.

The plant loop heating demand is distributed along the simulation period as shown in Fig. 3. From this approach, it could be noted that the main part of the demand is at low consume. Moreover, the number of hours at which the demand is higher than 4kWh only represents a 3.39% of the overall amount, in front of the resting 35.25%. The most common factor which enhances the low consume is that there is more demand under 1000Wh than over this value, 22.36% and 16.28%, respectively.



Zones mean air temperatures vs Outdoor air temperature

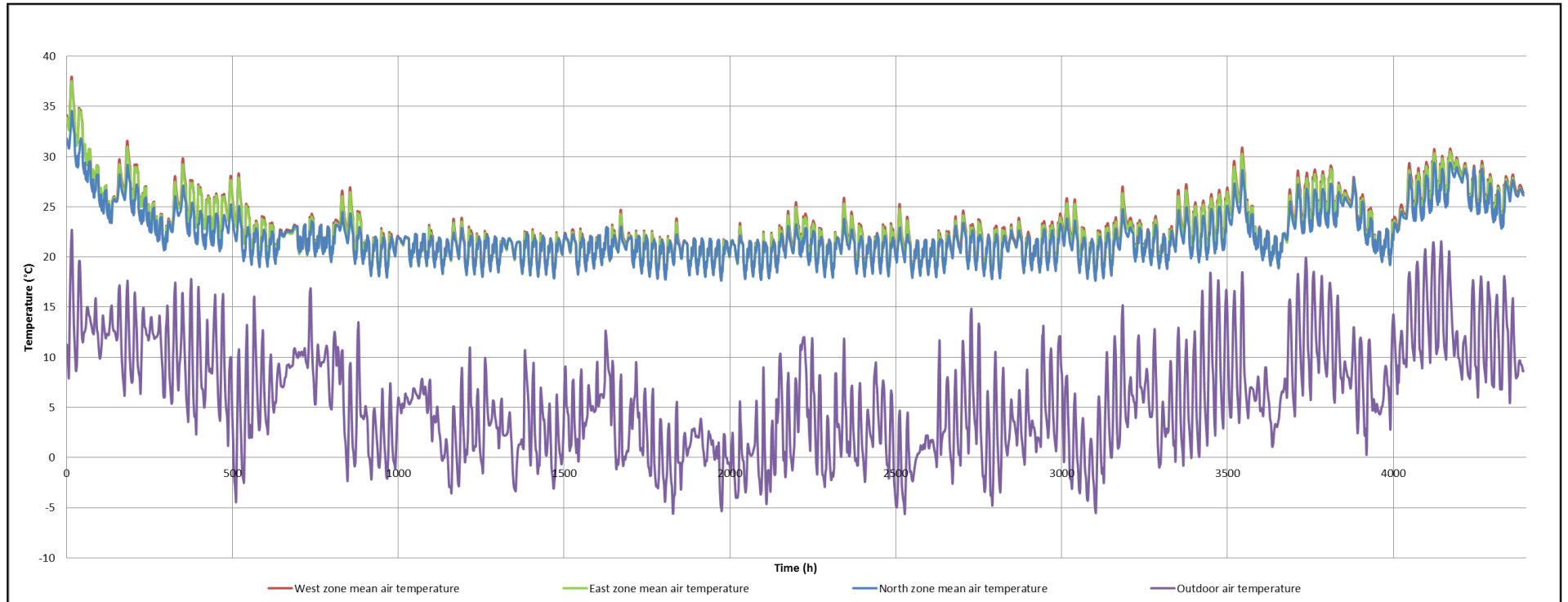


Figure 5. Plot of the mean air indoor and outdoor temperatures

Fig. 5 displays how the average temperature of three zones starts with a value as high as 35°C, to decrease until a value of approximately 20°C during the first 20 days (500h). Then, it remains constant during the cooler months and increases again around the middle of March.

The indoor temperature remains constant, without huge variations, after it is achieved at home (about 5°C between day and night). This is not the case of the outdoor temperature. Although its temperature profile is similar to the one displayed by the indoor temperature, the variation between two close instants reaches values of 15 or 20°C. The small indoor variations are not only due to the heating system, but also because of the insulation layers of walls, roof and ground which conserve the internal gains and reduce the heat losses. Other internal gains as lights, people and electric equipment also contribute to the indoor temperature.

Moreover, the confrontation of mean air temperatures for each zone reveals that the West zone has the highest temperature profile during the simulation period, followed by the East zone. Thus, the North zone, that is the coolest one, has lower temperatures most of the time. This is the reason why the North zone heating system is active more time than at the other zones and why there it is reached the highest value of total mass flow.

The total mass flow values consumed by the radiant panels are shown below in Table 14:

Table 14. Total mass flow values consumed by the radiant panels

Total mass flow consumption (kg/s)	
West zone	9.88
East zone	11.82
North zone	23.18

Approfondimento N. 3

Numerical comparison between energy and comfort performances of radiant heating and cooling systems versus air systems

Enrico Fabrizio, Stefano P. Corgnati, Francesco Causone and Marco Filippi

HVAC&R Research, 18(4):692–708, 2012. Copyright C _ 2012 ASHRAE.

ISSN: 1078-9669 print / 1938-5587 online

DOI: 10.1080/10789669.2011.578700

Abstract

A comparison between energy performance, simulated by means of the EnergyPlus building simulation program, of two air systems (all air and fan coil) and radiant heating and cooling floors/ceilings is developed in this work for various European climates (Milan, Frankfurt, London, Madrid, Athens, Helsinki, and Moscow) and carried out on a reference building selected from among U.S. Department of Energy commercial building new construction benchmarks. The comparison is focused on the analysis of energy sources and CO₂ emissions at equivalent thermal comfort quality levels in the various cases. The adoption of a radiant system, and of an appropriate primary energy system, always results in a reduction of energy sources exploited, of costs for energy wares purchased, and of carbon dioxide emissions. The greatest reductions can be achieved in climates where the energy demand for cooling is greater than the energy demand for heating. The article also focuses on the discussion of the procedure to be adopted when a comparison between air systems and radiant systems is implemented.

Introduction

Hydronic radiant panels represent a successful solution to be adopted if you want to achieve high thermal comfort levels and significant energy savings simultaneously. At the beginning, applications were for heating purposes, especially with radiation floor technologies; later, the use of radiant systems has been extended also to cooling purposes, and different solutions of radiant cooling floors and ceilings have been developed.

Nowadays, hydronic radiant panels are a consolidated climatization technology; they are widely used in Europe, and in North America, the number of applications is continuously increasing. As it is well known, the principles of radiant systems were already adopted in ancient times (Bean et al. 2010a), but only at the beginning of 1950s were they widely rediscovered and applied as building mechanical heating systems.

Mistakes, both in the design procedure and in the installation phase, have been done in some of the first applications (Feustel and Stetiu 1995; Bean et al. 2010b). These mistakes have generated a preliminary obstacle for the diffusion on the market of the radiant technique; on the other hand, they have stimulated the development of specific research addressed to the characterization of heat exchange mechanisms between the heating/cooling radiant surface and the surrounding indoor environment. Moreover, progress on the material science has allowed the adoption of safer and more flexible solutions aimed at providing easier installations, with plastic (polyethylene and polypropylene) pipes, modular radiant panels, etc. (Babiak et al. 2007) being used. At the same time, significant improvements have been carried out in the “theory of radiant climatization.” Dedicated design methods have been defined (Causone et al. 2010a) and dynamic energy simulation software tools have been developed or adapted to take into account the peculiarities of radiant systems (Strand and Pedersen 2002). The high comfort level provided in the indoor environment by radiant systems is a recognized successful feature (ASHARE 2007, 2008). In terms of thermal comfort, this is achieved by the preminent use of radiative heat exchanges between panel and occupants/walls (ASHARE 2007, 2008; Watson and Chapman 2002). To assure indoor air quality, radiant

systems are typically coupled with a dedicated outdoor air system (DOAS) (Causone and Corgnati, 2011; Jeong et al. 2003). A DOAS is an important element in radiant panel design. In fact, the ventilation system plays a fundamental role, because, in addition to guarantee the desired ventilation airflow rate, it keeps the humidity under control, avoiding condensation problems on the cooled surface of the panel (Conroy and Mumma 2001). Radiant panels can be used as the unique climatization system only when their heating/cooling capacity is higher than the total heating/cooling load. As their efficiency is limited by the maximum/minimum allowed surface temperature, when loads overcome the panel efficiency, the supplied ventilation air is coupled, especially in cooling mode (Jeong and Mumma 2006). As mentioned above, the great interest in radiant systems is due to the capability of maintaining high thermal comfort levels by using a fluid at a moderate temperature (low temperature heating and high temperature cooling; Babiak et al. 2007). This allows the exploitation of greater conversion efficiencies of primary energy systems (condensing boilers, heat pumps, liquid chilling packages, etc.). However, the actual energy savings depend strictly on the careful design and control of the radiant system, on the selection and sizing of the primary systems, on the climate, and on the other influencing boundary conditions (Olesen and Mattarolo 2009). The main aim of this work is to provide an assessment of the benefits that can be achieved by a radiant system in heating and cooling mode in terms of carbon dioxide emissions and energy savings, expressed in terms of delivered energy and source energy. This is done by means of a comparison between a system based on a radiant floor/ceiling for heating and cooling and a reference conventional all-air system, analyzed in various European climates. The performance of the systems is simulated by means of a building energy simulation program. [...]

Conclusioni

La ricerca oggetto di questo report è nella sua fase iniziale di sviluppo, per cui le conclusioni ed i risultati sinora ottenuti sono preliminari e rappresentano la base per i successivi approfondimenti ed analisi.

Nello specifico, i temi sviluppati nell'ambito del presente progetto hanno permesso di fornire una valutazione preliminare del potenziale incremento di prestazione ottenibile attraverso l'utilizzo di PCM fluidizzati in collettori solari e di porre le basi per la progettazione del sistema solare termico a slurry - PCM. E' stato preparato un profilo di domanda termica – per un ambiente residenziale – sulla base del quale si sta sviluppando l'attività progettuale che consentirà di realizzare un dimostratore sperimentale (in scala reale) ove testare sperimentalmente il sistema innovativo proposto. Questo profilo consentirà, oltre che sviluppare il dimensionamento dell'apparato di laboratorio, l'adeguata simulazione dell'utenza.

Parallelamente, si è preparato un modello numerico semplificato (operante su foglio Excel) per l'analisi del comportamento del sistema collettore – accumulo. Tale strumento di simulazione è stato poi utilizzato per condurre una analisi di sensibilità (al variare delle dimensioni del collettore solare dell'accumulo termico) del comportamento del sistema. Tale attività ha consentito di ottenere – congiuntamente al profilo temporale di domanda termica - le informazioni necessarie per il dimensionamento dei componenti del dimostratore.

In relazione ai risultati preliminari ottenuti, si osserva – come atteso – un aumento dell'efficienza del collettore grazie alle basse temperature medie del fluido operante TM. L'incremento prestazionale permette di soddisfare una maggiore domanda energetica rispetto all'acqua (domanda non soddisfatta pari al 34% per l'acqua e al 20% per il PCM).

L'energia accumulata aumenta del 18% circa grazie alla proprietà del fluido di assorbire più calore a bassa temperatura.

Il maggiore vantaggio nell'uso di una miscela di acqua e PCM risiede quindi nel fatto che è possibile un maggiore accumulo di energia.

Le successive analisi, in corso di preparazione e sviluppo, prevedono il test delle proprietà termofisiche degli slurry PCM in laboratorio ed un affinamento dello strumento di simulazione numerica del collettore solare e dell'accumulo. Si passerà quindi alla fase realizzativa del dimostratore.

Parallelamente, gli studi condotti sui pannelli radianti per la climatizzazione estiva hanno permesso di mettere in luce i significativi risparmi energetici conseguibili quando essi sono accoppiati a sistemi impiantistici a temperatura moderata.

Gli sviluppi futuri della ricerca condurranno alla verifica del funzionamento integrato di queste tecnologie costituenti il sistema edificio-impianto in particolare con riferimento alla presenza di significativi carichi solari.

Appendice

Marco Perino

Marco Perino was born the 7th of June 1963. He took his degree in Mechanical Engineering at the Polytechnic of Turin - Faculty of Engineering with a score of 110/110 summa cum laude.

In 1993 he took a PhD in Energy Technologies discussing a Thesis on small power combustion heat generators.

At the end of 1992 he won a researcher position at the 2nd Faculty of Engineering of the Polytechnic of Turin. From 1997 to the end of 2004 he was Associate professor at the Faculty of Architecture of the Polytechnic of Turin. On January 1st, 2005 he started his activity as a full professor at the first Faculty of Engineering at the Polytechnic of Turin.

During the years, he has given lectures on: thermal and HVAC systems, building physics, applied thermodynamic and heat transfer, control of the indoor environment, ventilation systems, thermal solar systems.

He is supervisory of about 5 Bachelor and 5 Master thesis per academic year and tutored various PhD students. Moreover, he was involved in the "Socrates/Erasmus" cooperation - EU project, delivering some lectures in different European Universities; in particular:

2000 - University of Eindhoven, The Netherland,

2005 - University of Stockholm (KTH) – Sweden,

2006 and 2007 - University of Aalborg – Denmark,

2009, 2011, 2012 - Istanbul Technical University (ITU) – Turkey.

Since 1° of April 2002, and for six months, he was visiting professor at the Aalborg University (AAU) in Denmark where he developed a joint research on themes related to natural ventilation and IAQ (single sided natural ventilation).

He participated, as "expert member", to the international research groups: "Annex 26 - Energy efficient ventilation of large enclosures", "Annex 35 - Hybrid Ventilation in New and Retrofitted Office Buildings" and "Annex 44 - Integrating environmentally responsive elements in buildings" (subtask leader of "responsive building elements") promoted by the International Energy Agency (IEA). He actively participated to project ESA-UNET (Subproject C: Energy Conservation in large Buildings), financed by the European Community, devoted to promote technical and scientific exchanges between European Universities and Universities of the South-East Asia.

He was member of a working group of the WHO (Natural ventilation for infection control in health-care settings) created to draft guidelines for the use of natural ventilation for infection control in health care settings.

He was/is responsible of more than 20 research/consultancy contracts of the Department of Energy of the Politecnico di Torino and of different research projects financed by the Italian Ministry of Education or Regional Authorities (in the years 2005 – 2012). He was the local responsible for the European Project – Marie Curie Training Network "CityNet" concerning energy conservation in building and energy planning at urban scale. Currently he is local responsible for the Intelligent Energy - Europe Project - "IDES-EDU". He participates to the European Project – Concerto "PolyCity" (energy retrofit of urban quarters).

he was member of the international working group of the ISIAQ Association "ISIAQ Task Force – Working group 21", which dealt with the indoor environment control in museums.

During the years the research activity of Marco Perino has been focused on the following subjects:

- small power heat appliances and combustion analysis,
- IAQ and pollutants dispersion inside confined spaces,
- air distribution and ventilation systems,
- HVAC systems and their thermofluidynamic analysis,
- domestic hoods,
- ventilation of large enclosures,
- natural and hybrid ventilation systems,
- experimental and theoretical analysis of single-side ventilation,

- indoor environment analysis/control in museums and historical buildings,
- thermofluidynamic analysis of traditional and innovative building envelope components,
- Indoor Environment Quality assessment,
- thermofluidynamic analysis and thermo-hygrometric control of museum showcases,

He was/is member of the Scientific Committee of the following conferences:

- AIVC 2008, 2010
- RoomVent 2007, 2009, 2011
- IAQVEC 2007 & 2010
- Indoor Air 2008
- IBPC – International Building Physics Conference 2009, 2012
- EERB-BEPH 2009 - The Fifth International Workshop on Energy and Environment of Residential Buildings
- Climate 2013.

He is reviewer for the following international journals: Energy and Buildings, Building and Environment, Indoor Air, Building Simulation, HVAC & Research, Journal of Power and Energy, Applied Thermal Energy.

He is AICARR (Italian Chapter of the ASHRAE Society), ASHRAE and ISIAQ (International Society of Indoor Air Quality) member.

He was member of the technical committee for the design of the showcase for the self-portrait of Leonardo and for the environmental monitoring during the temporary exhibition “Leonardo, il genio, il mito” at La Reggia della Venaria Reale.

The research activity is summarized in about 145 scientific papers published on national and international conference proceedings, national and international journals and books.

(publications list: <http://porto.polito.it/view/creators/Perino=3AMarco=3A002029=3A.html>)

Valentina Serra

Professor Valentina Serra graduated in Architecture at the Polytechnic of Turin in 1993 and received her PhD in 1998 in Building Physics. She was appointed Associate Professor of Building Physics in 2005.

She has been teaching different courses in the Faculty of Architecture on building physics and environmental control techniques for 15 years. She is actively involved in the management of the PhD course "Innovazione Tecnologica per l'Ambiente Costruito (Technology innovation for built environments) at the Polytechnic of Turin, where she is also a member of the academic board.

She has supervised about 140 Bachelor and Master thesis (mainly discussed at the School of Architecture) and tutored 4 PhD students.

Involved in national and international research projects and consultancy contracts with private companies and public organizations, her research activity has been mainly focused on the following subjects:

- numerical modeling and experimental analysis on energy performance of advanced transparent building component (i.e. advanced glazings, shading devices, responsive building elements, light ducts, green roofs);
- methods and tools for sustainable buildings design (she was involved in the drafting of the Guidelines for sustainable Olympic Villages in Torino 2006).

She participated, as “expert member”, to the international research groups:

Task 31 “Daylighting buildings in the 21st Century”, promoted by IEA-SHC(International Energy Agency Solar Heating &Cooling),

Annex 44 -Integrating environmentally responsive elements in buildings" promoted by IEA_ECBCS (International Energy Agency - Energy Conservation in Buildings and Community Systems)

She has been involved in the scientific board of Climamed 2007 International Conference and was chairman in CLIMAMED 2007 and COBEE 2008 international conference and in various national conference.

She is reviewer for the following international journals: Energy and Buildings, Building and Environment, Building Simulation, Journal of Architectural Science.

Results of base oriented research and applied research have been published in more than 70 papers.

(publications list: <http://porto.polito.it/view/creators/Serra=3AValentina=3A002179=3A.htm>)

Stefano Paolo Corgnati

Stefano Paolo Corgnati, graduated with honors in Mechanical Engineering and Ph.D in Energetics, is Associate Professor at the Energetics Department of the Politecnico di Torino, where he teaches building physics, building energy systems and sustainable building design at the 1st Faculty of Architecture. He works in the TEBE research group (www.polito.it/tebe) focusing on energy&buildings and indoor environmental control.

He is Vice-President of Rehva (Federation of HVAC European Associations) and member of Rehva Board of Directors.

He is member of the Directive Board of AICARR (Italian Association of Air Conditioning) and AICARR delegate for relations with Rehva.

He is the author of more than 180 scientific, technical and didactic publications, mainly concerning: radiant panels technologies, objective and subjective assessment of indoor environmental comfort, thermal mass activation techniques, energy certification and demand of existing buildings. For the quality of his research activity, he won in 2009 the Rehva “Young Scientist Award”. Moreover, in 2011 he was nominated “Rehva Fellow”.

He is involved in a number of National, European and International Research Projects on building energy consumptions.

He is sub-task leader of the research project Annex 53 “Total Energy Use in Buildings” of the International Energy Agency (IEA-ECBCS). He is chair of the REHVA Task Force on “Indoor Climate Quality Assessment”.

He is the operative manager of the Research Competence Centre TI-Green of Politecnico di Torino & Telecom about smart energy monitoring in buildings.

From 2008 to 2010, he was member of the Editorial Board of the Journal “CDA” (Condizionamentodell’Aria, Air Conditioning) and of the following “AICARR Journal”, official journals of AICARR.

In 2009 and 2010, he was coordinator of the working group of Politecnico di Torino aimed at supporting Piedmont Region for the implementation and application of Building Energy Certification.

Enrico Fabrizio

Enrico Fabrizio, born in Torino in 1978, graduated in Architecture at the Politecnico di Torino, PhD in Energetics at the Politecnico di Torino, PhD in Génie Civil at the Institut National des Sciences Appliquées de Lyon, since 2008 is assistant professor at the Department of Agricultural, Forestry and Environmental Economics and Engineering of the University of Torino.

From 2004 to 2007 he was PhD student and grant researcher at the Department of Energy of the Politecnico di Torino, and for some time in 2006 and 2007 at the Centre de Thermique de Lyon.

His research activities are based on the thermal building simulation, building energy systems modelling and optimization and RET.

He has been teaching thermal building physics and RET at both the Politecnico and the University of Torino. He has also been teaching environmental control for dairy housing at the Faculty of Agriculture of the University of Torino.

He his member of AICARR (Italian Association for Air Conditioning, Heating and Refrigeration), founding member and treasurer of IBPSA-Italy.

He has been reviewer for the following journals: Building and Environment, Energy and Buildings, Solar Energy, Applied Energy, Journal of Civil Engineering and Management, Energies, International Journal of Engineering Science and Technology, QScience Connect, Environmental Engineering and Management and for the Agence Nationale de la Recherche Française.

He has published 90 papers on applied researches. He is co-author of 14 research articles on the Energy and Buildings, Renewable and Sustainable Energy Reviews, Renewable Energy, Solar Energy, Building Simulation, Energy for Sustainable Development and HVAC&R Research journals.

He has written two books concerning the fundamentals (2012) and the applications (2005 and 2009) of the thermal building physics and has edited a guidebook on the dynamic thermal simulation (2012).

Fabio Favoino

Fabio Favoino is a born in Stigliano (MT) the 21 of August of 1986. He studied Building Engineering at the Engineering Faculty of Politecnico di Torino, where he conceived his BSc and MSc degree. During the MSc he took part to the LLP Erasmus program, attending architectural and engineering courses at the University of Technology of Delft (the Netherlands) for 6 months. He has a double master degree in Building Engineering (2010) at Politecnico di Torino and Politecnico di Milano, Alta Scuola Politecnica Diploma for Innovative projects in a multi-disciplinary setting (2010). His MSc thesis work won the 2010 prize as best thesis work from AICARR (Italian society of HVAC engineers), and was chosen by the AICARR to take part to the REHVA student competition.

He is currently a PhD student at the Energy Department of the Polytechnic University of Turin, under the supervision of Prof. Marco Perino. His research activity concerns innovative strategies, technologies and materials for dynamic and responsive building envelope systems for Zero Emission Building. Currently, his main activity deals with experimental evaluation of innovative façade modules (ACTRESS module – ACTIVE, RESPONSIVE and SOLAR module) characterized by the dynamic behavior and with on-board technologies for solar energy conversion and thermal storage.

Stefano Fantucci

Stefano Fantucci was born the 14th of February 1985. He took his degree in Architecture at the Polytechnic of Turin - with a score of 110/110 summa cum laude, discussing a thesis entitled: "TUBLOCK - High performance dry system for opaque envelopes" under the supervision of Prof.ssa Valentina Serra.

At the end of 2010, during his studies won the 6th edition of METRA prize, part of the workshop: "The technological project of architecture" Prof.ssa Gabriella Peretti, Prof. Orio De Paoli.

In 2011 he worked as a collaborator holder scholarship at LAMSA "Laboratory analysis and measurement of environmental system". carrying out activities to support teaching of the course "Design and quality certification for the energy efficiency of buildings" He received the title of: "Expert on the subject".

From 2010 to 2012 he worked at G-STUDIO Architects Enrico Giacobelli, as a collaborator to architectural design.

In the academic year 2011/2012 at Polytechnic of Turin, he worked as, assistant teaching to the following courses:

- Atelier : The architectural sustainable project - Building physics, Prof.ssa Valentina Serra, COURSE OF SUSTAINABLE PROJECT FOR ARCHITECTURE.

- Atelier : Sustainability in building-plant project - Environmental technology, Prof.ssa Valentina Serra, COURSE OF ARCHITECTURE FOR THE SUSTAINABILITY.

In 2012 he passed the exam to practice the profession of Architect, Registration of Landscape Architects Planners order in the province of Turin.

In 2012 he was/is Contract Professor teaching in the course of:

Architecture Laboratory - technology (module of Building physics), COURSE OF SCIENCE OF ARCHITECTURE.

In April 2012 he won a grant researcher position in "DENERG" Energy department of Polytechnic of Turin on "Technologies for Zero or Nearly Zero Energy Buildings".

Currently carries out the analysis and testing of advanced building envelope components